

The Veterinary Journal

Equine flexor tendon imaging part 2 – current status and future directions in advanced diagnostic imaging, with focus on the deep digital flexor tendon

--Manuscript Draft--

Manuscript Number:	YTVJL-D-21-00071R1
Article Type:	Invited review
Keywords:	computed tomography; horse; magnetic resonance imaging; tendinopathy
Corresponding Author:	Anna Ehrle, Dr. University of Liverpool Neston, Cheshire UNITED KINGDOM
First Author:	Anna Ehrle, Dr.
Order of Authors:	Anna Ehrle, Dr. Svenja Lilge, DVM Peter D. Clegg, Professor of Musculoskeletal Biology Thomas W. Maddox, BVSc PhD CertVDI DipECVDI MRCVS RCVS
Abstract:	Flexor tendon injuries are a common cause of lameness and early retirement in equine athletes. Whilst ultrasonography is most frequently utilized, advanced diagnostic imaging modalities are becoming more widely available for detection and monitoring of flexor tendon lesions. Part two of this literature review aims to detail the current experience with low- and high-field magnetic resonance imaging (MRI) and computed tomography (CT) for the diagnosis of equine flexor tendinopathy. Implications of the 'magic angle' artefact as well as injection techniques and the use of contrast are discussed. Besides lesion detection, future developments in tendon imaging focus on gaining enhanced structural information about the tendon architecture with the prospect to prevent injury. Techniques as described for the assessment of the human Achilles tendon including ultra-high field MRI and positron emission tomography are highlighted.

1 **Review**

2

3 **Equine flexor tendon imaging part 2 – current status and future directions in advanced**
4 **diagnostic imaging, with focus on the deep digital flexor tendon**

5

6

7 Anna Ehrle ^{a,b,*}, Svenja Lilge ^b, Peter D. Clegg ^a, Thomas W. Maddox ^{a,c}

8

9 ^a *Department of Musculoskeletal and Ageing Science, Institute of Life Course and Medical*

10 *Sciences, University of Liverpool, Liverpool L7 8TX, UK*

11 ^b *Equine Clinic, Freie Universität Berlin, 10965 Berlin, Germany*

12 ^c *Institute of Infection, Veterinary and Ecological Sciences, University of Liverpool, Neston*
13 *CH64 7TE, UK*

14

15

16

17

18 * Corresponding author. Tel.: +49 162 9146507.

19 E-mail address: annaehrle@googlemail.com (A. Ehrle).

20

21 **Abstract**

22 Flexor tendon injuries are a common cause of lameness and early retirement in equine
23 athletes. Whilst ultrasonography is most frequently utilized, advanced diagnostic imaging
24 modalities are becoming more widely available for detection and monitoring of flexor tendon
25 lesions. Part two of this literature review aims to detail the current experience with low- and
26 high-field magnetic resonance imaging (MRI) and computed tomography (CT) for the
27 diagnosis of equine flexor tendinopathy. ~~Implications of the~~ ~~Recently described approaches~~
28 ~~including~~ 'magic angle' ~~artefact~~ ~~MRI~~ as well as injection techniques and the use of contrast
29 are discussed. Besides lesion detection, future developments in tendon imaging focus on
30 gaining enhanced structural ~~and functional~~ information about the tendon architecture with the
31 prospect to prevent injury. Techniques as described ~~in~~ for the assessment of the human
32 Achilles tendon including ultra-high field MRI and positron emission tomography are
33 highlighted.

34
35 *Keywords:* Computed tomography; Horse; Magnetic resonance imaging; Tendinopathy
36

37 **Introduction**

38 ~~Superficial digital~~Equine flexor tendon (~~SDFT~~) injury is most commonly seen in
39 racing Thoroughbreds whereas injuries of the deep digital flexor tendon (DDFT) affect
40 horses performing in a wide variety of disciplines (Takahashi et al., 2004; Lam et al., 2007;
41 Smith et al., 2007; Arensburg et al., 2011). The majority of DDFT lesions involve the distal
42 aspect of the tendon and are associated with concurrent pathology of the
43 ~~podotrochlear/navicular~~ apparatus ~~and palmar foot pain~~ in approximately 51-79% of cases
44 (Blunden et al., 2006; Blunden et al., 2009; Vanel et al., 2012; Cillan-Garcia et al., 2013).
45 Clinical examination and ultrasonography are often sufficient for the diagnosis of SDFT
46 injury. The increasing availability of advanced diagnostic imaging modalities for the
47 assessment of the equine digit has however greatly improved the diagnosis of DDFT
48 pathology over the past two decades, particularly as the hoof capsule limits the utility of
49 ultrasonography in this area (Tucker and Sande, 2001; Mair and Kinns, 2005; Dyson and
50 Murray, 2007; Sherlock et al., 2015; Jones et al., 2019). For the second part of this review the
51 current literature was systematically assessed as described in review part 1 in order to provide
52 an overview of recent developments and future prospects for equine flexor tendon advanced
53 diagnostic imaging. The following search terms were used in PubMed, Medline and Google
54 Scholar without restrictions: 'tendon' AND 'magnetic resonance imaging' OR 'computed
55 tomography' AND 'equine' OR 'horse'. Additional studies were identified by searching the
56 reference list of eligible articles.

57
58 ~~Low-field~~ **Magnetic resonance imaging**

59 MRI for the evaluation of soft tissue injuries in equine patients was first introduced in
60 the early 1990s and has since become ~~widely used~~ the gold standard for tendon and ligament
61 imaging especially in the equine digit (Park et al., 1987; O'Callaghan, 1991; Denoix, 1994;

62 Kotani et al., 2000; King et al., 2013; Bubeck and Aarsvold, 2018). An increasing number of
63 low-field (0.25 ~~to- <1~~ Tesla) open MRI units are installed in equine referral practices across
64 Europe, the US and other countries, and several studies have proven a good correlation
65 between low- and high-field MR imaging findings and histopathological diagnosis of tendon
66 disease (~~Kasashima et al., 2002; Murray et al., 2004; Blunden et al., 2006; Murray et al.,~~
67 ~~2006; Blunden et al., 2009; Murray et al., 2009; Karlin et al., 2011; Sherlock et al., 2015)~~
68 (Table 1). Additionally, tendon injuries caused by foot penetrations or distal limb wounds can
69 be diagnosed with high accuracy using standing low-field MRI (del Junco et al., 2012;
70 Meehan, 2017; Schiavo et al., 2018; Sherlock et al., 2019).

71

72 Low-field MRI

Formatted: Font: Bold

73 *MR image acquisition: the 'magic angle'*

74 The 'magic angle' effect can impact on the interpretation of MR images depending on
75 the positioning of the limb in the magnetic field. The artefact is the result of~~characterized by~~
76 increased T2 relaxation times~~signal~~ that occurs when collagen fibres (which through strong
77 dipolar interaction typically have very low MR signal) are oriented at approximately 55° to
78 the main magnetic field (B₀) during image acquisition (Erickson et al., 1991; Erickson et al.,
79 1993; Bydder et al., 2007; Murray et al., 2009). The 'magic angle' effect typically manifests
80 as focally increased signal and is usually found on short echo time sequences including T1-
81 weighted fast spin echo and proton density-weighted sequences ~~but may also be observed on~~
82 ~~other sequences~~ (Peh and Chan, 1998; Li and Mirowitz, 2003; Richardson et al., 2018). The
83 common sites and appearance of the artefact are well documented for the DDFT ~~and~~
84 ligaments including the collateral ligaments of the distal interphalangeal joint (Spriet et al.,
85 2007; Smith et al., 2008; Spriet and McKnight, 2009; Spriet and Zwingerberger, 2009;
86 Gutierrez-Nibeyro et al., 2011). A recent report emphasized the importance of the position of

87 the long axis of the limb perpendicular to the magnetic field also for low-field MRI of the
88 SDFT. Leaning to one side as well as internal or external limb rotation during MR image
89 acquisition in the standing horse may create a 'magic angle' artefact in the SDFT at the level
90 of the pastern that should not be confused with tendon pathology (Fig. 1) (Sherlock and Mair,
91 2016).

92

93 *MRI for monitoring of tendon lesions*

94 Since MRI has been established as a sensitive tool for the diagnosis of tendinopathies
95 in the equine patient, the value of repeated MRI for monitoring purposes has been further
96 investigated. Sequential MRI evaluation of DDFT lesions in clinical cases has shown that
97 resolution of STIR-FSE and T2-FSE signal changes over time appear to be positive
98 prognostic indicators, whilst most lesions remain visible on T1-GRE and PD images even in
99 cases with excellent outcome (Holowinski et al., 2010; Vanel et al., 2012). Horses with T1-
100 GRE hyperintense DDFT lesions over 30mm in length or over 10% cross-sectional area, as
101 well as horses with persistent STIR-FSE signal or with concurrent lesions in the foot, are less
102 likely to return to their previous level of exercise (Dyson et al., 2005; Dyson and Murray,
103 2007; Vanel et al., 2012).

104

105 The ~~evolution~~development of different DDFT lesion types varies when assessed over
106 time. Dorsal border lesions showed a more rapid reduction in T2*-GRE volume and
107 ratiometric intensity (ratio between lesion and adjacent cortical bone) than parasagittal and
108 core lesions in clinical cases that were followed over a 6-month period (Milner et al., 2012).
109 No correlation between lameness and lesion signal intensity was found in this study, but
110 long-term telephone follow-up (18 months) of a larger group of horses confirmed that dorsal
111 border lesions seem to have a favourable prognosis for return to ~~some level of activity~~hidden

112 ~~exercise~~ (73%) when compared to other lesion types (core lesions 41%; parasagittal splits
113 50%) (Cillan-Garcia et al., 2013). However, overall only approximately 25% of these horses
114 returned to their previous level of exercise. ~~The~~^{is} study additionally showed an effect of
115 lesion location with a worse prognosis identified for insertional or suprasamoidean lesions
116 of the DDFT when compared to lesions at the level of the navicular bone. ~~That~~^{these} lesions
117 affecting both lobes of the DDFT ~~were~~^{are} not necessarily associated with a worse prognosis
118 than uniaxial defects (Cillan-Garcia et al., 2013).

119
120 Ultrasonography currently remains the most practical imaging modality for the
121 diagnosis and monitoring of SDFT lesions in a clinical setting (Bubeck and Aarsvold, 2018).
122 It is however important to note that the area of maximal cross-sectional injury in
123 experimentally induced SDFT lesions older than 4 weeks appears approximately 18% smaller
124 on ultrasonographic images when compared to standing low-field MRI (Schramme et al.,
125 2010; Karlin et al., 2011). Similar results were found in naturally occurring SDFT
126 lesions~~other studies~~ and should be taken into consideration when adjusting the exercise
127 program of a horse with SDFT tendinopathy based on ultrasonographic assessment alone
128 (~~Schramme et al., 2010~~; Berner et al., 2016). During sequential MRI examination, SDFT
129 lesions follow a pattern of signal change that differs from the pattern observed in DDFT
130 lesions over time. MR signal decreases earlier in T2-weighted images than in STIR-FSE
131 images in the SDFT (Schramme et al., 2010; Karlin et al., 2011; Berner et al., 2016; Berner,
132 2017; Berner et al., 2020).

134 **High-field MRI**

135 Most high-field MRI systems with a field strength of 1 Tesla (T) and above are
136 installed in larger referral centres. Examination is usually performed in a closed-bore magnet

137 and requires the horse to be anaesthetised (Lutter et al., 2015). Due to the higher signal-to-
138 noise ratio and corresponding increased image contrast and resolution, the tendon margins are
139 better defined, and subtle lesions appear more conspicuous on high-field MR images when
140 compared to standing low-field MRI (Ghazinoor et al., 2007; Murray et al., 2009). Whilst
141 tendon lesions and adhesions are generally detected on low- and high-field MR images, small
142 focal lesions (≤ 1 mm in diameter) and subtle dorsal fibrillation of the DDFT may be visible
143 on high-field MRI only (Murray et al., 2009).

144

145 *'Magic angle MRI'*

146 Similar to the appearance on low-field MRI where the B_0 magnetic field is oriented
147 vertically, the 'magic angle' effect at the distal aspect of the DDFT can be recognised mainly
148 on T1-weighted high-field MR images, when the long axis of the tendon is oriented at
149 approximately 55° ($\pm 5-7^\circ$) to the horizontally oriented static magnetic field (Busoni and
150 Snaps, 2002; Spriet and McKnight, 2009; Werpy et al., 2010). The artefact is characterised
151 by a hyperintense signal and can impact on the interpretation of MR images (Erickson et al.,
152 1991; Erickson et al., 1993). Since tendons generally present with little to no signal on MR
153 images, the intentional application of the 'magic angle' effect has been proposed to further
154 investigate the available signal of the tendon structure. The so called 'magic angle MRI'
155 allows sufficient signal to be obtained using the standard pulse sequences of clinical MRI
156 systems (Bydder et al., 2007). Using this technique, an increased T1 relaxation time has been
157 reported in cases of chronic Achilles tendinopathy in humans (Marshall et al., 2002; Oatridge
158 et al., 2003).

159

160 In an initial 'magic angle MRI' study on equine specimens, reference values for the
161 normal T1 relaxation times of the equine SDFT, DDFT and suspensory ligament were

162 determined (Spriet et al., 2011). To further assess possible changes in T1 relaxation
163 associated with tendinopathy, both laser-induced ~~and as well as~~ naturally occurring SDFT
164 lesions were subsequently evaluated (Spriet et al., 2012). All naturally occurring lesions were
165 visible on conventional as well as on ‘magic angle’ MR images. Based on the histological
166 findings the authors state however, that ‘magic angle MRI’ might be advantageous for the
167 identification of diffuse changes in tendon composition, that appeared hypointense on
168 conventional MR imaging (Spriet et al., 2012). Whilst the feasibility of ‘magic angle MRI’
169 has been demonstrated in high-and low-field MRI systems, the adequate positioning of the
170 limb may still prove to be a challenge in an *in vivo* setting (Spriet et al., 2012; Horstmeier et
171 al., 2019).

172

173 *Influence of local injection on MRI interpretation*

174 Research assessing the influence of diagnostic analgesia on MR image interpretation
175 showed that perineural analgesia of the palmar digital nerves, as well as intra-synovial
176 analgesia of the navicular bursa and the distal interphalangeal joint, do not significantly alter
177 MR images of the distal limb at 1.5 T (Black et al., 2013). Only the injection of 15 ml
178 mepivacaine into the digital flexor tendon sheath caused an iatrogenic increase in synovial
179 fluid volume as detected on MRI at 24 and 72 hours post injection (Black et al., 2013). The
180 study additionally described that needle tracts could not be appreciated consistently at any
181 injection site apart from the site of the navicular bursa injection, where some evidence for a
182 needle tract was detected in 10/15 limbs at 72 hours post injection.

183

184 Another study further investigated the influence of saline injection (30-35 ml) into the
185 digital flexor tendon sheath for the purpose of enhanced ultrasonographic and 1.5 T high-
186 field MR image interpretation (Daniel et al., 2019). The study showed that the presence of

187 fluid significantly improved the delineation of the DDFT in both imaging modalities and the
188 visualisation of the margins of the SDFT on MR images. As the technique did not introduce
189 any artefacts or altered the dimensions of the intra-thecal structures, further evaluation in
190 clinical cases should be of value particularly for the detection of marginal tendon lesions. It is
191 however important to consider that patients might be reluctant to stand during low-field MRI
192 following distention of the digital flexor tendon sheath. Consequently, the technique appears
193 to be more suited for high-field MR evaluation.

194
195 In order to facilitate assessment of the dorsal border of the DDFT at the level of the
196 navicular bone, the injection of the navicular bursa with saline (6-10 ml) or a mixture of
197 saline and contrast medium (5-6 ml, 1:1 ratio of 0.9% saline: Diatrizoate Meglumine and
198 Diatrizoate Sodium; Hypaque-76®) has been proposed (Schramme et al., 2009; Maher et al.,
199 2011). The distension of the navicular bursa physically separates the palmar surface of the
200 navicular bone from the dorsal margin of the DDFT and allows adhesions, DDFT fibrillation
201 and tendon splits at this level to be recognized more readily. The limitations of the technique
202 include the time required for the navicular bursa injection under radiographic guidance, and
203 the risk of rupture of the navicular bursa, especially if a volume in excess of 5 ml is injected
204 (Schramme et al., 2009; Maher et al., 2011). Alternatively, the distension of the distal
205 interphalangeal joint with saline (20-35 ml) alters the position of the proximal recess of the
206 navicular bursa and enhances the visualisation of the dorsal border of the DDFT, similar to
207 the direct approach to the navicular bursa (McGill et al., 2015). Both techniques are described
208 to be more reliable in the non-weightbearing limb when no pressure is exerted between the
209 navicular bone and the DDFT and are therefore probably more suitable for high-field MRI *in*
210 *vivo* (Maher et al., 2011; McGill et al., 2015).

211

212 *Contrast-enhanced MRI*

213 Gadolinium-based contrast-enhanced MRI is routinely performed ~~for~~ human and
214 small animal neurologic, oncologic and vascular imaging (Owen, 2018; Scott, 2018).
215 Gadolinium shortens the relaxation time constants (T1 and T2) of the tissues, which leads to
216 an increase in signal intensity, especially in T1-weighted images (Lin and Brown, 2007).
217 First clinical reports recommended an intra-venous gadopentate dimeglumine dose of 0.1
218 ml/kg (50 ml/horse) for musculoskeletal contrast-enhanced MRI in horses (Judy et al., 2008;
219 Saveraid and Judy, 2012; Daniel et al., 2013). The authors described the potential for an
220 improved recognition and assessment of tendon lesions, similar to the human Achilles
221 tendon, where a correlation between contrast enhancement and the severity of tendon lesions
222 has been demonstrated in a number of clinical cases (Shalabi et al., 2002; Richards et al.,
223 2010).

224
225 In order to decrease the volume and associated expense of gadolinium required for
226 contrast-enhanced MRI in horses, regional limb perfusion with gadopentate dimeglumine (5
227 ml in 5 ml 0.9% saline) via the palmar/plantar digital vein at the level of the mid
228 metacarpus/metatarsus was evaluated in a prospective clinical study (Aarsvold et al., 2018).
229 Pre- and post-contrast high-field (1.5 T) MRI was performed in anaesthetized horses in
230 lateral recumbency. C~~The~~ contrast enhancement in the distal limb was adequate provided the
231 tourniquet was secured in place. Multiple lesions were identified and were mostly visible on
232 pre-contrast as well as contrast-enhanced MR images. The authors describe, however, that the
233 technique aids the characterisation of lesions including adhesions and neovascularisation of
234 the DDFT (Aarsvold et al., 2018). In the standing horse the approach may be limited due to
235 difficulties in ensuring patients stand still for the requisite amount of time for the examination

236 post tourniquet application. Additionally, it might be challenging to replicate the exact
237 position of the foot in the magnet pre- and post contrast injection.
238

239 A further study compared systemic intra-venous injection with regional intra-arterial
240 injection of gadolinium in a group of horses with lameness localized to the foot (De Zani et
241 al., 2018). The injection of 0.02 ml/kg of gadolinium in the radial artery resulted in a higher
242 ratio of MRI contrast enhancement when compared to the systemic intra-venous route (0.1
243 ml/kg). Whilst the tendon tissue appeared generally not highly vascularised, significant
244 enhancement of the DDFT and peritendinous tissue was noted in the area of suspected
245 pathological lesions (De Zani et al., 2018).

246
247 The contrast enhancement in association with tendinopathy is most likely related to an
248 increased capillary permeability and diffusion of blood into the interstitial space in the acute
249 stages of the injury. Additionally, neovascularisation and granulation tissue formation are
250 suspected to show increased contrast uptake. However, histological studies of contrast-
251 enhancing lesion in the equine distal limb are currently lacking (Shalabi et al., 2002; Saveraid
252 and Judy, 2012; Nelson et al., 2017).

253
254 Side effects of the administration of gadolinium-based contrast agents are described in
255 human and small animal patients, but no severe adverse reactions were encountered in the
256 aforementioned equine studies (Wible et al., 2001; Grobner and Prischl, 2007; Lin and
257 Brown, 2007; Girard and Leece, 2010; Saveraid and Judy, 2012; Prince et al., 2017; Aarsvold
258 et al., 2018; De Zani et al., 2018). A recent review of the use of contrast media in horses
259 classified the risk associated with the administration of gadolinium generally as low,
260 provided horses do not suffer underlying renal disease or dehydration (Nelson et al., 2017).

261 Future research should further ascertain the benefits of contrast-enhanced over standard MRI
262 for the assessment of tendon lesions and identify how imaging findings correlate with
263 histopathology. Additionally, the combined approach of contrast-enhanced and ‘magic angle
264 MRI’ as described for the human Achilles tendon might be of interest for equine flexor
265 tendon imaging (Marshall et al., 2002).

266

267 **Ultra-high field MRI**

268 The high-field MRI systems currently installed in veterinary centres for clinical
269 applications operate at a field strength of 1.5 to 3 T. Magnets used in humans for clinical
270 purposes have now reached 7 T, and preclinical research ultra-high field MRI systems
271 exceeding a field strength of 10 T are available (Alizai et al., 2018; Ladd et al., 2018).

272

273 Low- and high-field MRI facilitates the detection and assessment of tendon lesions,
274 but the visualisation of the tendon structure remains difficult. The very short transverse
275 relaxation time of normal tendon tissue, with the relatively long echo times used in
276 conventional clinical MRI sequences usually result in the complete decay of tendon signal
277 before it can be sampled (Juras et al., 2012; Guidetti et al., 2018; Juras et al., 2019). With
278 increasing field strength and signal-to-noise ratio, and the use of ultrashort echo time (UTE)
279 and other sequences, MR images of the finer tendon structural components can be obtained
280 (Fig. 2) (Robson et al., 2004; Du et al., 2010; Moser et al., 2012; Juras et al., 2013; Chang et
281 al., 2015; Foure, 2016). In man, ultra-high field MRI is utilized to visualise the fascicular
282 pattern of the Achilles tendon *in vivo* (Han et al., 2014; Foure, 2016; Juras et al., 2019).

283

284 *Ultra-high field MRI of the equine SDFT*

285 Ultra-high field MRI (9.4 T) of the equine SDFT facilitates the detailed assessment of
286 the tendon structure with clear delineation of the tendon fascicles and interfascicular matrix
287 (Fig. 2 A + B). Additionally, T2*-weighted 3D-FISP gradient echo transverse images provide
288 a comprehensive picture for the characterisation of tendon lesions (Fig. 2C). At this stage the
289 size of the radiofrequency coil and the time required to obtain this high level of anatomical
290 detail preclude the *in vivo* assessment of tendon lesions in horses. The cost and technical
291 expertise involved with MR imaging at higher field strength limits its availability in
292 veterinary medicine, however, ultra-high field MRI offers promising prospects for
293 musculoskeletal imaging as clinical progress continues (Alizai et al., 2018; Ladd et al., 2018).

294

295 **Computed tomography**

296 The limited availability of MRI has led to the investigation of alternative modalities
297 for soft tissue advanced diagnostic imaging in equine orthopaedics (Tucker and Sande, 2001;
298 Puchalski, 2012; Jones et al., 2019). A study comparing MRI and CT for the assessment of
299 the equine distal limb found similar scores for the visibility of the DDFT in the area of the
300 pastern for both modalities, but the distal DDFT at the level of insertion showed better
301 visualisation scores with low-field MRI (Vallance et al., 2012a). Likewise, the classification
302 of DDFT lesions varies depending on the imaging modality used for interpretation. More
303 lesions of the distal DDFT were detected with low-field MRI but lesions at the level of the
304 pastern as well as abrasions and mineralisation of the DDFT were more likely to be
305 diagnosed with CT in a cohort of clinical cases (Fig. 3) (Vallance et al., 2012b). Additional
306 reports comparing both, MRI and CT imaging findings of the same subject with results of
307 histopathological examination would give further insight and support image interpretation
308 (Whitton et al., 1998; Puchalski et al., 2009).

309

310 *Contrast-enhanced computed tomography*

311 The contrast media used for CT studies in equine patients are usually iodinated
312 solutions that strongly attenuate X-rays and highlight areas of increased vascular perfusion or
313 permeability (Bushberg et al., 2012; Nelson et al., 2017). Following acquisition of pre-
314 contrast images the intra-vascular or intra-thecal route of administration may be chosen for
315 contrast-enhanced CT imaging of the equine distal limb (Puchalski, 2012; Nelson et al.,
316 2017).

317
318 There are some reports of intra-venous contrast studies in the horse (Hunter et al.,
319 2016; Walker et al., 2017). However, the technique most commonly described is the regional
320 intra-arterial injection of contrast medium, including placement of a catheter in the medial
321 palmar artery at the level of the carpometacarpal joint under ultrasonographic guidance in the
322 anaesthetised horse. Steady-state infusion of a 1:1 dilution of ionic-iodinated contrast in
323 saline is subsequently maintained with a remotely controlled pressure injector (2 ml/s),
324 starting 3-5 seconds prior to CT examination (Collins et al., 2004; Puchalski et al., 2005;
325 Puchalski et al., 2007; Puchalski et al., 2009; Pollard and Puchalski, 2011b). Whilst tendon
326 lesions are less common in the hindlimb, contrast application via catheterisation of the lateral
327 dorsal metatarsal artery is also described (van Hamel et al., 2014) (Fig. 4). The normal CT
328 anatomy and attenuation values for tendon and ligament before and after intra-arterial
329 contrast administration have been documented in detail (Tietje et al., 2001; Puchalski et al.,
330 2007; Vallance et al., 2012a; Claerhoudt et al., 2014). The DDFT generally shows a slight but
331 significant increase in post-contrast attenuation (8-17 HU) that potentially impairs on the
332 clear anatomical visualisation of the tendon (Puchalski et al., 2007; Vallance et al., 2012a).

333

334 DDFT lesions in the area of the foot are usually characterised by marked contrast
335 enhancement (> 20 HU) that may be central, peripheral or diffuse (Puchalski et al., 2009;
336 Puchalski, 2011; Vallance et al., 2012b; van Hamel et al., 2014). Lack of contrast
337 enhancement has been occasionally observed in dorsal border lesions of the DDFT. A
338 sensitivity of 93% for lesion detection was determined following histopathological
339 examination of the affected tissue in one study (van Hamel et al., 2014). All false negative
340 results obtained in this study were at the level of the navicular bone where the visibility of the
341 DDFT is most limited on CT images (Vallance et al., 2012a; van Hamel et al., 2014). Clinical
342 studies have shown that lesions of the DDFT can also be diagnosed based on non-contrast-
343 enhanced CT (Tietje et al., 2001; Jones et al., 2019). However, lesions in the area of the
344 DDFT insertion were more likely to be identified post-contrast in one study (Vallance et al.,
345 2012b).

346
347 CT contrast tenography may aid the evaluation of the flexor tendons as they course
348 through the digital flexor tendon sheath (Fig. 54). Consistent delineation of the flexor tendon
349 borders and the *manica flexoria* has been described after intra-theal injection of nonionic-
350 iodinated contrast solution (60 ml) into the digital flexor tendon sheath of cadaver limbs
351 without flexor tendon pathology (Lacitignola et al., 2015; Agass et al., 2018). Further
352 research should confirm the value of this technique for diagnostic purposes and pre-surgical
353 planning.

354
355 Adverse reactions to the intravascular administration of iodinated contrast are rare in
356 horses but may include a transient increase in heart rate and blood pressure as well as local or
357 generalised skin reactions (Gunkel et al., 2004; Pollard and Puchalski, 2011a; Nelson et al.,
358 2017). CT technology is advancing rapidly and the resolution of images obtained for the

359 assessment of clinical cases has considerably increased over the past decade (Puchalski,
360 2012; Riggs, 2018). High slice number multidetector CT scanners are becoming more widely
361 available and first examples of distal limb examination in standing horses have been reported
362 (Desbrosse et al., 2008; Koch et al., 2020; [Mageed 2020](#); [Pauwels et al., 2021](#)). In contrast to
363 MR imaging, CT does not offer the capability of accurately detecting the fluid content
364 within a tendon lesion to date. However, with its improved image quality and fast acquisition
365 time, CT may provide a practical alternative to MRI for advanced diagnostic imaging of the
366 equine flexor tendons (Riggs, 2018; Jones et al., 2019). Future research should show whether
367 CT imaging is comparable to MRI regarding the assessment of lesion progression over time.
368 Additionally, patient tolerance regarding contrast procedures in the standing horse warrants
369 further investigation.

370

371 *Positron emission tomography*

372 Positron Emission tomography (PET) is a nuclear medicine imaging technique mainly
373 used in the field of human oncology, but orthopaedic applications are also described in man
374 (Fischer et al., 2010; Fischer, 2013; Kim et al., 2015; Eliasson et al., 2016; Aide et al., 2019).
375 In contrast to gamma scintigraphy where planar images are obtained after the injection of a
376 radioactive agent, PET acquires cross-sectional images allowing for three-dimensional
377 assessment of the region of interest (Spriet, 2019). PET is usually combined with CT in order
378 to obtain functional and structural information. As this setup is currently difficult to realise in
379 large patients like horses, a PET scanner used for preclinical brain research has been adapted
380 for PET imaging of the equine distal limb. First reports of PET imaging in equine
381 orthopaedics mainly describe the benefits of the technique for the detection of osseous lesions
382 and enthesopathy (Spriet et al., 2016; Spriet et al., 2018; Spriet et al., 2019; Norvall et al.,
383 2020). PET imaging has been applied for the monitoring of the healing response after

384 Achilles tendon rupture in human patients and increased uptake of the glucose tracer ¹⁸F-
385 fluorodeoxyglucose was detected in horses with SDFT and DDFT tendinopathy in one
386 exploratory study (Eliasson et al., 2016; Spriet et al., 2016). Future studies will further
387 determine the value of PET imaging for the assessment of the equine flexor tendons in
388 clinical cases (Spriet, 2019).

389

390 **Conclusion**

391 The rapid and ongoing technological progress and particularly the influence of
392 modern computing has led to the development of a multitude of approaches for soft tissue
393 imaging. Not all techniques described in preclinical studies or human orthopaedic research
394 will be economical or practical enough to be carried through into veterinary clinical
395 diagnostics. However, the last two decades have shown how fast advanced diagnostic
396 imaging modalities including MRI and CT have been integrated in equine orthopaedics at
397 referral level. Both modalities have benefits and disadvantages, particularly for the
398 assessment of flexor tendon injuries. Detailed knowledge of MRI and CT approaches
399 including the implications of the ‘magic angle’ and the use of injection techniques and
400 contrast should aid image interpretation and selection of the appropriate modality. As
401 diagnostic imaging is crucial for the diagnosis and monitoring of equine tendinopathy and
402 ~~potentially aids has high potential for~~ the prevention of tendon injury, there is ongoing
403 demand for future studies in this developing field of research.

404

405 **Conflict of interest statement**

406 None of the authors has any financial or personal relationships that could
407 inappropriately influence or bias the content of the paper.

408

409 **Acknowledgements**

410 The authors gratefully acknowledge the assistance of Dr. Carolin Müller and Birte
411 Drees (Lucidity Diagnostics) with the preparation of the figures.

412

413 **References:**

- 414 Aarsvold, S., Solano, M., Garcia-Lopez, J., 2018. Magnetic resonance imaging following
415 regional limb perfusion of gadolinium contrast medium in 26 horses. *Equine*
416 *Veterinary Journal* 50, 649-657.
- 417
- 418 Agass, R., Dixon, J., Fraser, B., 2018. Computed tomographic contrast tenography of the
419 digital flexor tendon sheath of the equine hindlimb. *Veterinary Radiology &*
420 *Ultrasound* 59, 279-288.
- 421
- 422 Aide, N., Hicks, R.J., Le Tourneau, C., Lheureux, S., Fanti, S., Lopci, E., 2019. FDG
423 PET/CT for assessing tumour response to immunotherapy : report on the EANM
424 symposium on immune modulation and recent review of the literature. *European*
425 *Journal of Nuclear Medicine and Molecular Imaging* 46, 238-250.
- 426
- 427 Alizai, H., Chang, G., Regatte, R.R., 2018. MR imaging of the musculoskeletal system using
428 ultrahigh field (7T) MR imaging. *PET Clinics* 13, 551-565.
- 429
- 430 Arensburg, L., Wilderjans, H., Simon, O., Dewulf, J., Boussauw, B., 2011. Nonseptic
431 tenosynovitis of the digital flexor tendon sheath caused by longitudinal tears in the
432 digital flexor tendons: a retrospective study of 135 tenoscopic procedures. *Equine*
433 *Veterinary Journal* 43, 660-668.
- 434
- 435 Berner, D., Brehm, W., Gerlach, K., Gittel, C., Offhaus, J., Paebst, F., Scharner, D., Burk, J.,
436 2016. Longitudinal cell tracking and simultaneous monitoring of tissue regeneration
437 after cell treatment of natural tendon disease by low-field magnetic resonance
438 imaging. *Stem Cells International*, 1207190.
- 439
- 440 Berner, D., 2017. Diagnostic imaging of tendinopathies of the superficial flexor tendon in
441 horses. *The Veterinary Record* 181, 652-654.
- 442
- 443 Berner, D., Brehm, W., Gerlach, K., Offhaus, J., Scharner, D., Burk, J., 2020. Variation in the
444 MRI signal intensity of naturally occurring equine superficial digital flexor
445 tendinopathies over a 12-month period. *The Veterinary Record* 187, e53.
- 446
- 447 Black, B., Cribb, N.C., Nykamp, S.G., Thomason, J.J., Trout, D.R., 2013. The effects of
448 perineural and intrasynovial anaesthesia of the equine foot on subsequent magnetic
449 resonance images. *Equine Veterinary Journal* 45, 320-325.
- 450
- 451 Blunden, A., Dyson, S., Murray, R., Schramme, M., 2006. Histopathology in horses with
452 chronic palmar foot pain and age-matched controls. Part 2: the deep digital flexor
453 tendon. *Equine Veterinary Journal* 38, 23-27.
- 454

455 Blunden, A., Murray, R., Dyson, S., 2009. Lesions of the deep digital flexor tendon in the
456 digit: a correlative MRI and post mortem study in control and lame horses. *Equine*
457 *Veterinary Journal* 41, 25-33.

458

459 Bubeck, K.A., Aarsvold, S., 2018. Diagnosis of soft tissue injury in the sport horse.
460 *Veterinary Clinics of North America: Equine Practice* 34, 215-234.

461

462 Bushberg, J.T., Seibert, J.A., Leidholdt, E.M., Boone, J.M., 2012. Interaction of radiation
463 with matter. In: *The Essential Physics of Medical Imaging*. Third Edn. Lippincott,
464 Williams & Wilkins, Philadelphia, PA, USA, pp. 33-59.

465

466 Busoni, V., Snaps, F., 2002. Effect of deep digital flexor tendon orientation on magnetic
467 resonance imaging signal intensity in isolated equine limbs-the magic angle effect.
468 *Veterinary Radiology & Ultrasound* 43, 428-430.

469

470 Bydder, M., Rahal, A., Fullerton, G.D., Bydder, G.M., 2007. The magic angle effect: a source
471 of artifact, determinant of image contrast, and technique for imaging. *Journal of*
472 *Magnetic Resonance Imaging* 25, 290-300.

473

474 Chang, E.Y., Du, J., Chung, C.B., 2015. UTE imaging in the musculoskeletal system. *Journal*
475 *of Magnetic Resonance Imaging* 41, 870-883.

476

477 Cillan-Garcia, E., Milner, P.I., Talbot, A., Tucker, R., Hendey, F., Boswell, J., Reardon, R.J.,
478 Taylor, S.E., 2013. Deep digital flexor tendon injury within the hoof capsule; does
479 lesion type or location predict prognosis? *The Veterinary Record* 173, 70.

480

481 Claerhoudt, S., Bergman, E.H., Saunders, J.H., 2014. Computed tomographic anatomy of the
482 equine foot. *Anatomia Histologia Embryologia* 43, 395-402.

483

484 Collins, J.N., Galuppo, L.D., Thomas, H.L., Wisner, E.R., Hornof, W.J., 2004. Use of
485 computed tomography angiography to evaluate the vascular anatomy of the distal
486 portion of the forelimb of horses. *American Journal of Veterinary Research* 65, 1409-
487 1420.

488

489 Daniel, A.J., Judy, C.E., Saveraid, T., 2013. Magnetic resonance imaging of the
490 metacarpo(tarso)phalangeal region in clinically lame horses responding to diagnostic
491 analgesia of the palmar nerves at the base of the proximal sesamoid bones: five cases.
492 *Equine Veterinary Education* 25, 222-228.

493

494 Daniel, A.J., Leise, B.S., Selberg, K.T., Barrett, M.F., 2019. Enhanced ultrasonographic
495 imaging of the equine distal limb using saline injection of the digital flexor tendon
496 sheath: a cadaver study. *The Veterinary Journal* 247, 26-31.

497

498 De Zani, D., Rabbogliatti, V., Ravasio, G., Pettinato, C., Giancamillo, M.D., Zani, D.D.,
499 2018. Contrast enhanced magnetic resonance imaging of the foot in horses using
500 intravenous versus regional intraarterial injection of gadolinium. *Open Veterinary*
501 *Journal* 8, 471-478.

502

503 del Junco, C.I., Mair, T.S., Powell, S.E., Milner, P.I., Font, A.F., Schwarz, T., Weaver, M.P.,
504 2012. Magnetic resonance imaging findings of equine solar penetration wounds.
505 *Veterinary Radiology & Ultrasound* 53, 71-75.
506

507 Denoix, J.-M., 1994. Diagnostic techniques for identification and documentation of tendon
508 and ligament injuries. *Veterinary Clinics of North America: Equine Practice* 10, 365-
509 407.
510

511 Desbrosse, F.G., Vandeweerd, J.M.E.F., Perrin, R.A.R., Clegg, P.D., Launois, M.T.,
512 Brogniez, L., Gehin, S.P., 2008. A technique for computed tomography (CT) of the
513 foot in the standing horse. *Equine Veterinary Education* 20, 93-98.
514

515 Du, J., Chiang, A.J., Chung, C.B., Statum, S., Znamirovski, R., Takahashi, A., Bydder,
516 G.M., 2010. Orientational analysis of the Achilles tendon and entheses using an
517 ultrashort echo time spectroscopic imaging sequence. *Magnetic Resonance Imaging*
518 28, 178-184.
519

520 Dyson, S., Murray, R., 2007. Magnetic resonance imaging evaluation of 264 horses with foot
521 pain: the podotrochlear apparatus, deep digital flexor tendon and collateral ligaments
522 of the distal interphalangeal joint. *Equine Veterinary Journal* 39, 340-343.
523

524 Dyson, S.J., Murray, R., Schramme, M.C., 2005. Lameness associated with foot pain: results
525 of magnetic resonance imaging in 199 horses (January 2001-December 2003) and
526 response to treatment. *Equine Veterinary Journal* 37, 113-121.
527

528 Eliasson, P., Couppe, C., Lonsdale, M., Svensson, R.B., Neergaard, C., Kjaer, M., Friberg,
529 L., Magnusson, S.P., 2016. Ruptured human Achilles tendon has elevated metabolic
530 activity up to 1 year after repair. *European Journal of Nuclear Medicine and*
531 *Molecular Imaging* 43, 1868-1877.
532

533 Erickson, S.J., Cox, I.H., Hyde, J.S., Carrera, G.F., Strandt, J.A., Estkowski, L.D., 1991.
534 Effect of tendon orientation on MR imaging signal intensity: a manifestation of the
535 "magic angle" phenomenon. *Radiology* 181, 389-392.
536

537 Erickson, S.J., Prost, R.W., Timins, M.E., 1993. The "Magic angle" effect: background
538 physics and clinical relevance. *Radiology* 188, 23-25.
539

540 Fischer, D.R., Maquieira, G.J., Espinosa, N., Zanetti, M., Hesselmann, R., Johayem, A.,
541 Hany, T.F., von Schulthess, G.K., Strobel, K., 2010. Therapeutic impact of
542 [(18)F]fluoride positron-emission tomography/computed tomography on patients with
543 unclear foot pain. *Skeletal Radiology* 39, 987-997.
544

545 Fischer, D.R., 2013. Musculoskeletal imaging using fluoride PET. *Seminars in Nuclear*
546 *Medicine* 43, 427-433.
547

548 Foure, A., 2016. New imaging methods for non-invasive assessment of mechanical,
549 structural, and biochemical properties of human Achilles tendon: a mini review.
550 *Frontiers in Physiology* 7, 324.
551

552 Ghazinoor, S., Crues, J.V., 3rd, Crowley, C., 2007. Low-field musculoskeletal MRI. *Journal*
553 *of Magnetic Resonance Imaging* 25, 234-244.
554

555 Girard, N.M., Leece, E.A., 2010. Suspected anaphylactoid reaction following intravenous
556 administration of a gadolinium-based contrast agent in three dogs undergoing
557 magnetic resonance imaging. *Veterinary Anaesthesia and Analgesia* 37, 352-356.
558

559 Grobner, T., Prischl, F.C., 2007. Gadolinium and nephrogenic systemic fibrosis. *Kidney*
560 *International* 72, 260-264.
561

562 Guidetti, M., Zampini, M.A., Gandini, G., Gupta, A., Li, W., Magin, R.L., Wang, V.M.,
563 2018. Diffusion tensor imaging of tendons and ligaments at ultra-high magnetic
564 fields. *Critical Reviews in Biomedical Engineering* 46, 311-339.
565

566 Gunkel, C.I., Valverde, A., Robertson, S.A., Thompson, M.S., Keoughan, C.G., Ferrell, E.A.,
567 2004. Treatment for a severe reaction to intravenous administration of diatrizoate in
568 an anesthetized horse. *Journal of the American Veterinary Medical Association* 224,
569 1143-1146.
570

571 Gutierrez-Nibeyro, S.D., Werpy, N.M., White, N.A., 2nd, McCutcheon, J., Weng, H.Y.,
572 Christopher, J.M., 2011. Standing low-field magnetic resonance imaging appearance
573 of normal collateral ligaments of the equine distal interphalangeal joint. *Veterinary*
574 *Radiology & Ultrasound* 52, 521-533.
575

576 Han, M., Larson, P.E., Liu, J., Krug, R., 2014. Depiction of Achilles tendon microstructure in
577 vivo using high-resolution 3-dimensional ultrashort echo-time magnetic resonance
578 imaging at 7 T. *Investigative Radiology* 49, 339-345.
579

580 Holowinski, M., Judy, C., Saveraid, T., Maranda, L., 2010. Resolution of lesions on STIR
581 images is associated with improved lameness status in horses. *Veterinary Radiology*
582 *& Ultrasound* 51, 479-484.
583

584 Horstmeier, C., Ahrberg, A.B., Berner, D., Burk, J., Gittel, C., Hillmann, A., Offhaus, J.,
585 Brehm, W., 2019. In vivo magic angle magnetic resonance imaging for cell tracking
586 in equine low-field MRI. *Stem Cells International* 2019, 1-9.
587

588 Hunter, B.G., Huber, M.J., Nemanic, S., 2016. The use of computed tomography to diagnose
589 bilateral forelimb tendon pathology in a horse with unilateral lameness. *Equine*
590 *Veterinary Education* 28, 439-443.
591

592 Jones, A.R.E., Ragle, C.A., Mattoon, J.S., Sanz, M.G., 2019. Use of non-contrast-enhanced
593 computed tomography to identify deep digital flexor tendinopathy in horses with
594 lameness: 28 cases (2014-2016). *Journal of the American Veterinary Medical*
595 *Association* 254, 852-858.
596

597 Judy, C.E., Saveraid, R.C., Rodgers, E.H., Rick, M.C., Herthel, D.J., 2008. Characterization
598 of foot lesions using contrast enhanced equine orthopedic magnetic resonance
599 imaging. In: *Proceedings of the 54th Annual Convention of the American Association*
600 *of Equine Practitioners, San Diego, California, USA, 6th-10th December 2008*, p.
601 459.

602
603 Juras, V., Welsch, G., Bar, P., Kronnerwetter, C., Fujita, H., Trattnig, S., 2012. Comparison
604 of 3T and 7T MRI clinical sequences for ankle imaging. *European Journal of*
605 *Radiology* 81, 1846-1850.
606
607 Juras, V., Apprich, S., Szomolanyi, P., Bieri, O., Deligianni, X., Trattnig, S., 2013. Bi-
608 exponential T2 analysis of healthy and diseased Achilles tendons: an in vivo
609 preliminary magnetic resonance study and correlation with clinical score. *European*
610 *Radiology* 23, 2814-2822.
611
612 Juras, V., Mlynarik, V., Szomolanyi, P., Valkovic, L., Trattnig, S., 2019. Magnetic resonance
613 imaging of the musculoskeletal system at 7T: morphological imaging and beyond.
614 *Topics in Magnetic Resonance Imaging* 28, 125-135.
615
616 Karlin, W.M., Stewart, A.A., Durgam, S.S., Naughton, J.F., O'Dell-Anderson, K.J., Stewart,
617 M.C., 2011. Evaluation of experimentally induced injury to the superficial digital
618 flexor tendon in horses by use of low-field magnetic resonance imaging and
619 ultrasonography. *American Journal of Veterinary Research* 72, 791-798.
620
621 Kasashima, Y., Kuwano, A., Katayama, Y., Taura, Y., Yoshihara, T., 2002. Magnetic
622 resonance imaging application to live horse for diagnosis of tendinitis. *Journal of*
623 *Veterinary Medical Science* 64, 577-582.
624
625 Kim, J.Y., Choi, Y.Y., Kim, Y.H., Park, S.B., Jeong, M.A., 2015. Role of (18)F-fluoride
626 PET/CT over dual-phase bone scintigraphy in evaluation and management of lesions
627 causing foot and ankle pain. *Annals of Nuclear Medicine* 29, 302-312.
628
629 King, J.N., Zubrod, C.J., Schneider, R.K., Sampson, S.N., Roberts, G., 2013. MRI findings in
630 232 horses with lameness localized to the metacarpo(tarso)phalangeal region and
631 without a radiographic diagnosis. *Veterinary Radiology & Ultrasound* 54, 36-47.
632
633 Koch, C., Pauwels, F.E., Schweizer-Gorgas, D., 2020. Technical set-up and case illustration
634 of orthopaedic cone beam computed tomography in the standing horse. *Equine*
635 *Veterinary Education*, (Epub ahead of print) doi: 10.1111/eve.13290.
636
637 Kotani, H., Taura, Y., Sakai, A., Tsuka, T., Kageyama, Y., Nakaichi, M., 2000. Antemortem
638 evaluation for magnetic resonance imaging of the equine flexor tendon. *Journal of*
639 *Veterinary Medical Science* 62, 81-84.
640
641 Lacitignola, L., De Luca, P., Guarracino, A., Crovace, A., 2015. Computed tomographic
642 tenography of normal equine digital flexor tendon sheath: an ex vivo study.
643 *Veterinary Medicine International* 2015, 903169.
644
645 Ladd, M.E., Bachert, P., Meyerspeer, M., Moser, E., Nagel, A.M., Norris, D.G., Schmitter,
646 S., Speck, O., Straub, S., Zaiss, M., 2018. Pros and cons of ultra-high-field MRI/MRS
647 for human application. *Progress in Nuclear Magnetic Resonance Spectroscopy* 109, 1-
648 50.
649

- 650 Lam, K.H., Parkin, T.D.H., Riggs, C.M., Morgan, K.L., 2007. Descriptive analysis of
651 retirement of Thoroughbred racehorses due to tendon injuries at the Hong Kong
652 Jockey Club (1992-2004). *Equine Veterinary Journal* 39, 143-148.
653
- 654 Li, T., Mirowitz, S.A., 2003. Manifestation of magic angle phenomenon: comparative study
655 on effects of varying echo time and tendon orientation among various MR sequences.
656 *Magnetic Resonance Imaging* 21, 741-744.
657
- 658 Lin, S.P., Brown, J.J., 2007. MR contrast agents: physical and pharmacologic basics. *Journal*
659 *of Magnetic Resonance Imaging* 25, 884-899.
660
- 661 Lutter, J.D., Schneider, R.K., Sampson, S.N., Cary, J.A., Roberts, G.D., Vahl, C.I., 2015.
662 Medical treatment of horses with deep digital flexor tendon injuries diagnosed with
663 high-field-strength magnetic resonance imaging: 118 cases (2000–2010). *Journal of*
664 *the American Veterinary Medical Association* 247, 1309-1318.
665
- 666 [Mageed, M., 2020. Standing computed tomography of the equine limb using a multi-slice
667 helical scanner: Technique and feasibility study. *Equine Veterinary Education*. \(Epub
668 ahead of print\) doi: 10.1111/eve.13388](#)
669
- 670 Maher, M.C., Werpy, N.M., Goodrich, L.R., McIlwraith, C.W., 2011. Positive contrast
671 magnetic resonance bursography for assessment of the navicular bursa and
672 surrounding soft tissues. *Veterinary Radiology & Ultrasound* 52, 385-393.
673
- 674 Mair, T.S., Kinns, J., 2005. Deep digital flexor tendonitis in the equine foot diagnosed by
675 low-field magnetic resonance imaging in the standing patient: 18 cases. *Veterinary*
676 *Radiology & Ultrasound* 46, 458-466.
677
- 678 Marshall, H., Howarth, C., Larkman, D.J., Herlihy, A.H., Oatridge, A., Bydder, G.M., 2002.
679 Contrast-enhanced magic-angle MR imaging of the Achilles tendon. *American*
680 *Journal of Roentgenology* 179, 187-192.
681
- 682 McGill, S.L., Gutierrez-Nibeyro, S.D., Schaeffer, D.J., Hartman, S.K., O'Brien, R.T., Joslyn,
683 S.K., 2015. Saline arthrography of the distal interphalangeal joint for low-field
684 magnetic resonance imaging of the equine podotrochlear bursa: feasibility study.
685 *Veterinary Radiology & Ultrasound* 56, 417-424.
686
- 687 Meehan, L., 2017. Should I use magnetic resonance imaging to evaluate horses with foot
688 penetrations? *Equine Veterinary Education* 29, 521-522.
689
- 690 Milner, P.I., Sidwell, S., Talbot, A.M., Clegg, P.D., 2012. Short-term temporal alterations in
691 magnetic resonance signal occur in primary lesions identified in the deep digital
692 flexor tendon of the equine digit. *Equine Veterinary Journal* 44, 157-162.
693
- 694 Moser, E., Stahlberg, F., Ladd, M.E., Trattnig, S., 2012. 7-T MR-from research to clinical
695 applications? *NMR in Biomedicine* 25, 695-716.
696
- 697 Murray, R.C., Roberts, B.L., Schramme, M.C., Dyson, S.J., Branch, M., 2004. Quantitative
698 evaluation of equine deep digital flexor tendon morphology using magnetic resonance
699 imaging. *Veterinary Radiology & Ultrasound* 45, 103-111.

- 700
701 Murray, R.C., Blunden, T.S., Schramme, M.C., Dyson, S.J., 2006a. How does magnetic
702 resonance imaging represent histologic findings in the equine digit? *Veterinary*
703 *Radiology & Ultrasound* 47, 17-31.
- 704
705 Murray, R.C., Schramme, M.C., Dyson, S.J., Branch, M.V., Blunden, T.S., 2006b. Magnetic
706 resonance imaging characteristics of the foot in horses with palmar foot pain and
707 control horses. *Veterinary Radiology & Ultrasound* 47, 1-16.
- 708
709 Murray, R.C., Mair, T.S., Sherlock, C.E., Blunden, A.S., 2009. Comparison of high-field and
710 low-field magnetic resonance images of cadaver limbs of horses. *The Veterinary*
711 *Record* 165, 281-288.
- 712
713 Nelson, B.B., Goodrich, L.R., Barrett, M.F., Grinstaff, M.W., Kawcak, C.E., 2017. Use of
714 contrast media in computed tomography and magnetic resonance imaging in horses:
715 techniques, adverse events and opportunities. *Equine Veterinary Journal* 49, 410-424.
- 716
717 Norvall, A., Spriet, M., Espinosa, P., Arino-Estrada, G., Murphy, B.G., Katzman, S.A.,
718 Galuppo, L.D., 2020. Chondrosesamoidean ligament enthesopathy: prevalence and
719 findings in a population of lame horses imaged with positron emission tomography.
720 *Equine Veterinary Journal*, (Epub ahead of print) doi: 10.1111/evj.13299.
- 721
722 O'Callaghan, M.W., 1991. Future diagnostic methods. A brief look at new technologies and
723 their potential application to equine diagnosis. *Veterinary Clinics of North America:*
724 *Equine Practice* 7, 467-479.
- 725
726 Oatridge, A., Herlihy, A., Thomas, R.W., Wallace, A.L., Puri, B.K., Larkman, D.J., Bydder,
727 G.M., 2003. Magic angle imaging of the Achilles tendon in patients with chronic
728 tendonopathy. *Clinical Radiology* 58, 384-388.
- 729
730 Owen, M., 2018. Radiographic, computed tomography, and magnetic resonance contrast
731 media. In: *Textbook of Veterinary Diagnostic Radiology*. Seventh Edn. Elsevier
732 Saunders, St. Louis, MO, USA, pp. 96-109.
- 733
734 Park, R.D., Nelson, T.R., Hoopes, P.J., 1987. Magnetic resonance imaging of the normal
735 equine digit and metacarpophalangeal joint. *Veterinary Radiology* 28, 105-116.
- 736
737 Pauwels, F.E., Van der Vekens, E., Christan, Y., Koch, C., Schweizer, D., 2021. Feasibility,
738 indications, and radiographically confirmed diagnoses of standing extremity cone
739 beam computed tomography in the horse. *Veterinary Surgery* 50, 365-374.
- 740
741 Peh, W.C.G., Chan, J.H.M., 1998. The magic angle phenomenon in tendons: effect of
742 varying the MR echo time. *British Journal of Radiology* 71, 31-36.
- 743
744 Pollard, R., Puchalski, S., 2011a. CT contrast media and applications. In: *Veterinary*
745 *Computed Tomography*. First Edn. Wiley Blackwell, Sussex, UK, pp. 57-65.
- 746
747 Pollard, R.E., Puchalski, S.M., 2011b. Reaction to intraarterial ionic iodinated contrast
748 medium administration in anesthetized horses. *Veterinary Radiology & Ultrasound*
749 52, 441-443.

Formatted: English (United States)

Formatted: German (Germany)

Formatted: English (United Kingdom)

750
751 Prince, M.R., Lee, H.G., Lee, C.H., Youn, S.W., Lee, I.H., Yoon, W., Yang, B., Wang, H.,
752 Wang, J., Shih, T.T., et al., 2017. Safety of gadobutrol in over 23.000 patients: the
753 GARDIAN study, a global multicentre, prospective, non-interventional study.
754 *European Radiology* 27, 286-295.
755
756 Puchalski, S.M., Snyder, J.R., Hornof, W.J., Macdonald, M.H., Galuppo, L.D., 2005.
757 Contrast-enhanced computed tomography of the equine distal extremity. In:
758 Proceedings of the 51th Annual Convention of the American Association of Equine
759 Practitioners, Seattle, Washington, USA, 3rd-7th December 2005, pp. 389-394.
760
761 Puchalski, S.M., Galuppo, L.D., Hornof, W.J., Wisner, E.R., 2007. Intraarterial contrast-
762 enhanced computed tomography of the equine distal extremity. *Veterinary Radiology*
763 & *Ultrasound* 48, 21-29.
764
765 Puchalski, S.M., Galuppo, L.D., Drew, C.P., Wisner, E.R., 2009. Use of contrast-enhanced
766 computed tomography to assess angiogenesis in deep digital flexor tendonopathy in a
767 horse. *Veterinary Radiology & Ultrasound* 50, 292-297.
768
769 Puchalski, S., 2011. Equine foot. In: *Veterinary Computed Tomography*. First Edn. Wiley
770 Blackwell, Sussex, UK, pp. 463-471.
771
772 Puchalski, S.M., 2012. Advances in equine computed tomography and use of contrast media.
773 *Veterinary Clinics of North America: Equine Practice* 28, 563-581.
774
775 Richards, P.J., McCall, I.W., Day, C., Belcher, J., Maffulli, N., 2010. Longitudinal
776 microvascularity in Achilles tendinopathy (Power Doppler ultrasound, magnetic
777 resonance imaging time-intensity curves and the Victorian Institute of Sport
778 Assessment-Achilles questionnaire): a pilot study. *Skeletal Radiology* 39, 509-521.
779
780 Richardson, M.L., Amini, B., Richards, T.L., 2018. Some new angles on the magic angle:
781 what MSK radiologists know and don't know about this phenomenon. *Skeletal*
782 *Radiology* 47, 1673-1681.
783
784 Riggs, C.M., 2018. Computed tomography in equine orthopaedics – the next great leap?
785 *Equine Veterinary Education* 31, 151-153.
786
787 Robson, M.D., Benjamin, M., Gishen, P., Bydder, G.M., 2004. Magnetic resonance imaging
788 of the Achilles tendon using ultrashort TE (UTE) pulse sequences. *Clinical Radiology*
789 59, 727-735.
790
791 Saveraid, T.C., Judy, C.E., 2012. Use of intravenous gadolinium contrast in equine magnetic
792 resonance imaging. *Veterinary Clinics of North America: Equine Practice* 28, 617-
793 636.
794
795 Schiavo, S., Cillan-Garcia, E., Elce, Y., Liuti, T., Taylor, S.E., 2018. Horses with solar foot
796 penetration, deep digital flexor tendon injury, and absence of concurrent synovial
797 sepsis can have a positive outcome. *Veterinary Radiology & Ultrasound* 59, 697-704.
798

799 Schramme, M., Kerekes, Z., Hunter, S., Nagy, K., Pease, A., 2009. Improved identification of
800 the palmar fibrocartilage of the navicular bone with saline magnetic resonance
801 bursography. *Veterinary Radiology & Ultrasound* 50, 606-614.
802
803 Schramme, M., Kerekes, Z., Hunter, S., Labens, R., 2010. Mr imaging features of surgically
804 induced core lesions in the equine superficial digital flexor tendon. *Veterinary*
805 *Radiology & Ultrasound* 51, 280-287.
806
807 Scott, L.J., 2018. Gadobutrol: A review in contrast-enhanced MRI and MRA. *Clinical Drug*
808 *Investigation* 38, 773-784.
809
810 Shalabi, A., Kristoffersen-Wiberg, M., Papadogiannakis, N., Aspelin, P., Movin, T., 2002.
811 Dynamic contrast-enhanced mr imaging and histopathology in chronic Achilles
812 tendinosis. A longitudinal MR study of 15 patients. *Acta Radiologica* 43, 198-206.
813
814 Sherlock, C.E., Mair, T.S., Ireland, J., Blunden, T., 2015. Do low field magnetic resonance
815 imaging abnormalities correlate with macroscopical and histological changes within
816 the equine deep digital flexor tendon? *Research in Veterinary Science* 98, 92-97.
817
818 Sherlock, C.E., Mair, T.S., 2016. Magic angle effect on low field magnetic resonance images
819 in the superficial digital flexor tendon in the equine proximal pastern region. *The*
820 *Veterinary Journal* 217, 126-131.
821
822 Sherlock, C., Fairburn, A., Lawson, A., Mair, T., 2019. The use of magnetic resonance
823 imaging for the assessment of distal limb wounds in horses: A pilot study. *Equine*
824 *Veterinary Education* 32, 637-645.
825
826 Smith, M.R., Wright, I.M., Smith, R.K., 2007. Endoscopic assessment and treatment of
827 lesions of the deep digital flexor tendon in the navicular bursae of 20 lame horses.
828 *Equine Veterinary Journal* 39, 18-24.
829
830 Smith, M.A., Dyson, S.J., Murray, R.C., 2008. Is a magic angle effect observed in the
831 collateral ligaments of the distal interphalangeal joint or the oblique sesamoidean
832 ligaments during standing magnetic resonance imaging? *Veterinary Radiology &*
833 *Ultrasound* 49, 509-515.
834
835 Spriet, M., Mai, W., McKnight, A., 2007. Asymmetric signal intensity in normal collateral
836 ligaments of the distal interphalangeal joint in horses with a low-field MRI system
837 due to the magic angle effect. *Veterinary Radiology & Ultrasound* 48, 95-100.
838
839 Spriet, M., McKnight, A., 2009. Characterization of the magic angle effect in the equine deep
840 digital flexor tendon using a low-field magnetic resonance system. *Veterinary*
841 *Radiology & Ultrasound* 50, 32-36.
842
843 Spriet, M., Zwingerberger, A., 2009. Influence of the position of the foot on MRI signal in
844 the deep digital flexor tendon and collateral ligaments of the distal interphalangeal
845 joint in the standing horse. *Equine Veterinary Journal* 41, 498-503.
846

- 847 Spriet, M., Wisner, E.R., Anthenill, L.A., Buonocore, M.H., 2011. Determination of T1
848 relaxation time of normal equine tendons using magic angle magnetic resonance
849 imaging. *Veterinary Radiology & Ultrasound* 52, 149-153.
- 850
851 Spriet, M., Murphy, B., Vallance, S.A., Vidal, M.A., Whitcomb, M.B., Wisner, E.R., 2012.
852 Magic angle magnetic resonance imaging of diode laser induced and naturally
853 occurring lesions in equine tendons. *Veterinary Radiology & Ultrasound* 53, 394-401.
- 854
855 Spriet, M., Espinosa, P., Kyme, A.Z., Stepanov, P., Zavarzin, V., Schaeffer, S., Katzman,
856 S.A., Galuppo, L.D., Beylin, D., 2016. Positron emission tomography of the equine
857 distal limb: exploratory study. *Veterinary Radiology & Ultrasound* 57, 630-638.
- 858
859 Spriet, M., Espinosa, P., Kyme, A.Z., Phillips, K.L., Katzman, S.A., Galuppo, L.D.,
860 Stepanov, P., Beylin, D., 2018. ¹⁸F-sodium fluoride positron emission tomography of
861 the equine distal limb: Exploratory study in three horses. *Equine Veterinary Journal*
862 50, 125-132.
- 863
864 Spriet, M., 2019. PETting horses? *Equine Veterinary Journal* 51, 283-284.
- 865
866 Spriet, M., Espinosa-Mur, P., Cissell, D.D., Phillips, K.L., Arino-Estrada, G., Beylin, D.,
867 Stepanov, P., Katzman, S.A., Galuppo, L.D., Garcia-Nolen, T., et al., 2019. ¹⁸F-
868 sodium fluoride positron emission tomography of the racing Thoroughbred fetlock:
869 validation and comparison with other imaging modalities in nine horses. *Equine*
870 *Veterinary Journal* 51, 375-383.
- 871
872 Takahashi, T., Kasashima, Y., Ueno, Y., 2004. Association between race history and risk of
873 superficial digital flexor tendon injury in Thoroughbred racehorses. *Journal of the*
874 *American Veterinary Medical Association* 225, 90-93.
- 875
876 Tietje, S., Nowak, M., Petzoldt, S., Weiler, H., 2001. Computed tomographic evaluation of
877 the distal aspect of the deep digital flexor tendon (DDFT) in horses. *Pferdeheilkunde*
878 17, 21-29.
- 879
880 Tucker, R.L., Sande, R.D., 2001. Computed tomography and magnetic resonance imaging in
881 equine musculoskeletal conditions. *Veterinary Clinics of North America: Equine*
882 *Practice* 17, 145-157.
- 883
884 Vallance, S.A., Bell, R.J., Spriet, M., Kass, P.H., Puchalski, S.M., 2012a. Comparisons of
885 computed tomography, contrast enhanced computed tomography and standing low-
886 field magnetic resonance imaging in horses with lameness localised to the foot. Part
887 1: anatomic visualisation scores. *Equine Veterinary Journal* 44, 51-56.
- 888
889 Vallance, S.A., Bell, R.J., Spriet, M., Kass, P.H., Puchalski, S.M., 2012b. Comparisons of
890 computed tomography, contrast-enhanced computed tomography and standing low-
891 field magnetic resonance imaging in horses with lameness localised to the foot. Part
892 2: Lesion identification. *Equine Veterinary Journal* 44, 149-156.
- 893
894 van Hamel, S.E., Bergman, H.J., Puchalski, S.M., de Groot, M.W., van Weeren, P.R., 2014.
895 Contrast-enhanced computed tomographic evaluation of the deep digital flexor tendon

896 in the equine foot compared to macroscopic and histological findings in 23 limbs.
897 Equine Veterinary Journal 46, 300-305.
898
899 Vanel, M., Olive, J., Gold, S., Mitchell, R.D., Walker, L., 2012. Clinical significance and
900 prognosis of deep digital flexor tendinopathy assessed over time using MRI.
901 Veterinary Radiology & Ultrasound 53, 621-627.
902
903 Walker, W.T., Ducharme, N.G., Tran, J., Scrivani, P.V., 2017. Nonselective computed
904 tomography angiography for detecting arterial blood flow to the distal limb following
905 trauma in two small equids. Equine Veterinary Education 29, 15-21.
906
907 Werpy, N.M., Ho, C.P., Kawcak, C.E., 2010. Magic angle effect in normal collateral
908 ligaments of the distal interphalangeal joint in horses imaged with a high-field
909 magnetic resonance imaging system. Veterinary Radiology & Ultrasound 51, 2-10.
910
911 Whitton, R.C., Buckley, C., Donovan, T., Wales, A.D., Dennis, R., 1998. The diagnosis of
912 lameness associated with distal limb pathology in a horse: a comparison of
913 radiography, computed tomography and magnetic resonance imaging. The Veterinary
914 Journal 155, 223-229.
915
916 Wible, J.H., Galen, K.P., Wojdyla, J.K., 2001. Cardiovascular effects caused by rapid
917 administration of gadoversetamide injection in anesthetized dogs. Investigative
918 Radiology 36, 292-298.
919

920 **Table 1**
 921 Overview of the literature validating magnetic resonance imaging (MRI) in the equine distal
 922 limb for the assessment of the superficial digital flexor tendon (SDFT) and the deep digital
 923 flexor tendon (DDFT).

<u>Low-field MRI</u>	<u>Literature source</u>	<u>Area examined</u>	<u>No of horses</u>
<u>0.2 T</u>	<u>Kasashima et al., 2002</u>	<u>SDFT</u>	<u>6</u>
<u>0.27 T</u>	<u>Murray et al. 2009</u>	<u>SDFT / DDFT</u>	<u>10</u>
<u>0.25 T</u>	<u>Karlin et al., 2011</u>	<u>SDFT</u>	<u>8</u>
<u>0.27 T</u>	<u>Sherlock et al., 2015</u>	<u>DDFT</u>	<u>26</u>
<u>High-field MRI</u>			
<u>1.5 T</u>	<u>Murray et al., 2004</u>	<u>DDFT (distal)</u>	<u>38</u>
<u>1.5 T</u>	<u>Murray et al., 2006a</u>	<u>DDFT (distal)</u>	<u>32</u>
<u>1.5 T</u>	<u>Murray et al., 2006b</u>	<u>DDFT (distal)</u>	<u>34</u>
<u>1.5 T</u>	<u>Murray et al., 2009</u>	<u>SDFT / DDFT</u>	<u>10</u>
<u>1.5 T</u>	<u>Blunden et al., 2006</u>	<u>DDFT (distal)</u>	<u>32</u>
<u>1.5 T</u>	<u>Blunden et al., 2009</u>	<u>DDFT (distal)</u>	<u>46</u>

924

925 **Figure legends**

926 Fig 1. T1-weighted gradient echo (GRE) FAST transverse low-field (0.27T) magnetic
927 resonance image of the equine distal limb at proximal pastern level (lateral is to the left/right).
928 (A) Note the increased T2 signal intense ‘magic angle’ artefact at the mid- to lateral aspect of
929 the superficial digital flexor tendon (SDFT) (black arrow) as observed with ‘leaning in’ or
930 lateral rotation of the limb during image acquisition. (B) lesion of the medial lobe of the
931 SDFT (white arrow) (Image courtesy of Birte Drees, Lucidity Diagnostics 2020).

932
933 Fig. 2. T2*-weighted 3D-FISP (fast imaging with steady-state free precession) gradient echo
934 transverse MR images of the superficial digital flexor tendon (lateral is to the left). (A) 3-year
935 old Irish Sports Horse mare without pre-existing orthopaedic condition. (B) 25-year old
936 Thoroughbred mare without a history of orthopaedic disease. Thinning of the interfascicular
937 matrix is evident as a result of ageing. (C) 8-year old Thoroughbred gelding with clinical SDFT
938 tendinopathy.

939
940 Fig. 3. Transverse computed tomographic (CT) images (soft tissue window without contrast)
941 of the deep digital flexor tendon (DDFT) at the level of the lower pastern (lateral is to the
942 left). (A) Longitudinal split of the lateral lobe of the DDFT (white arrow) with moderate
943 distension of the navicular bursa (black arrow). (B) Dorsal border lesion of the DDFT (white
944 arrow) (Images courtesy of Carolin Müller, Lucidity Diagnostics 2020).

945
946 Fig. 4. Contrast enhanced computed tomographic images (bone window) showing the deep
947 digital flexor tendon (DDFT) of the left hindlimb of a 10-year-old Warmblood showjumper,
948 acquired during steady-state infusion of ionic-iodinated contrast in saline (1:1; 2ml/s) via the
949 lateral dorsal metatarsal artery (lateral is to the left). (A) Note the increased contrast

950 enhancement associated with a core lesion of the DDFT in zone 4B (white arrow). (B)
951 Additionally, perilesional contrast attenuation was evident in both lobes of the DDFT in zone
952 P2A (white arrows) in the same horse.

953
954 Fig. 54. Computed tomographic (CT) images of the flexor tendons at the level of the digital
955 flexor tendon sheath with (B + D) and without (A + C) intra-theal application of nonionic-
956 iodinated contrast. The superficial and deep digital flexor tendons can be recognized on
957 transverse (A) and sagittal (C) CT images using the soft tissue window. The outline of the
958 *manica flexoria* (white arrow) and the flexor tendons is highlighted following injection of the
959 digital flexor tendon sheath with contrast (B + D) (lateral is to the left on Fig. 5 A and B)
960 (Images courtesy of Carolin Müller, Lucidity Diagnostics 2020).

1 **Review**

2

3 **Equine flexor tendon imaging part 2 – current status and future directions in advanced**
4 **diagnostic imaging, with focus on the deep digital flexor tendon**

5

6

7 Anna Ehrle ^{a,b,*}, Svenja Lilge ^b, Peter D. Clegg ^a, Thomas W. Maddox ^{a,c}

8

9 ^a *Department of Musculoskeletal and Ageing Science, Institute of Life Course and Medical*
10 *Sciences, University of Liverpool, Liverpool L7 8TX, UK*

11 ^b *Equine Clinic, Freie Universität Berlin, 10965 Berlin, Germany*

12 ^c *Institute of Infection, Veterinary and Ecological Sciences, University of Liverpool, Neston*
13 *CH64 7TE, UK*

14

15

16

17

18 * Corresponding author. Tel.: +49 162 9146507.

19 *E-mail address:* annaehrle@googlemail.com (A. Ehrle).

20

21 **Abstract**

22 Flexor tendon injuries are a common cause of lameness and early retirement in equine
23 athletes. Whilst ultrasonography is most frequently utilized, advanced diagnostic imaging
24 modalities are becoming more widely available for detection and monitoring of flexor tendon
25 lesions. Part two of this literature review aims to detail the current experience with low- and
26 high-field magnetic resonance imaging (MRI) and computed tomography (CT) for the
27 diagnosis of equine flexor tendinopathy. Implications of the ‘magic angle’ artefact as well as
28 injection techniques and the use of contrast are discussed. Besides lesion detection, future
29 developments in tendon imaging focus on gaining enhanced structural information about the
30 tendon architecture with the prospect to prevent injury. Techniques as described for the
31 assessment of the human Achilles tendon including ultra-high field MRI and positron
32 emission tomography are highlighted.

33

34 *Keywords:* Computed tomography; Horse; Magnetic resonance imaging; Tendinopathy

35

36 **Introduction**

37 Superficial digital flexor tendon (SDFT) injury is most commonly seen in racing
38 Thoroughbreds whereas injuries of the deep digital flexor tendon (DDFT) affect horses
39 performing in a wide variety of disciplines (Takahashi et al., 2004; Lam et al., 2007; Smith et
40 al., 2007; Arensburg et al., 2011). The majority of DDFT lesions involve the distal aspect of
41 the tendon and are associated with concurrent pathology of the podotrochlear apparatus in
42 approximately 51-79% of cases (Blunden et al., 2006; Blunden et al., 2009; Vanel et al.,
43 2012; Cillan-Garcia et al., 2013). Clinical examination and ultrasonography are often
44 sufficient for the diagnosis of SDFT injury. The increasing availability of advanced
45 diagnostic imaging modalities for the assessment of the equine digit has however greatly
46 improved the diagnosis of DDFT pathology over the past two decades, particularly as the
47 hoof capsule limits the utility of ultrasonography in this area (Tucker and Sande, 2001; Mair
48 and Kinns, 2005; Dyson and Murray, 2007; Sherlock et al., 2015; Jones et al., 2019). For the
49 second part of this review the current literature was systematically assessed as described in
50 review part 1 in order to provide an overview of recent developments and future prospects for
51 equine flexor tendon advanced diagnostic imaging. The following search terms were used in
52 PubMed, Medline and Google Scholar without restrictions: ‘tendon’ AND ‘magnetic
53 resonance imaging’ OR ‘computed tomography’ AND ‘equine’ OR ‘horse’. Additional
54 studies were identified by searching the reference list of eligible articles.

55

56 **Magnetic resonance imaging**

57 MRI for the evaluation of soft tissue injuries in equine patients was first introduced in
58 the early 1990s and has since become widely used for tendon and ligament imaging
59 especially in the equine digit (Park et al., 1987; O'Callaghan, 1991; Denoix, 1994; Kotani et
60 al., 2000; King et al., 2013; Bubeck and Aarsvold, 2018). An increasing number of low-field

61 (0.25 to <1 Tesla) open MRI units are installed in equine referral practices across Europe, the
62 US and other countries, and several studies have proven a good correlation between low- and
63 high-field MR imaging findings and histopathological diagnosis of tendon disease (Table 1).
64 Additionally, tendon injuries caused by foot penetrations or distal limb wounds can be
65 diagnosed with high accuracy using standing low-field MRI (del Junco et al., 2012; Meehan,
66 2017; Schiavo et al., 2018; Sherlock et al., 2019).

67

68 **Low-field MRI**

69 *MR image acquisition: the 'magic angle'*

70 The 'magic angle' effect can impact on the interpretation of MR images depending on
71 the positioning of the limb in the magnetic field. The artefact is the result of increased T2
72 relaxation time that occurs when collagen fibres (which through strong dipolar interaction
73 typically have very low MR signal) are oriented at approximately 55° to the main magnetic
74 field (B₀) during image acquisition (Erickson et al., 1991; Erickson et al., 1993; Bydder et al.,
75 2007; Murray et al., 2009). The 'magic angle' effect typically manifests as focally increased
76 signal and is usually found on short echo time sequences including T1-weighted fast spin
77 echo and proton density-weighted sequences (Peh and Chan, 1998; Li and Mirowitz, 2003;
78 Richardson et al., 2018). The common sites and appearance of the artefact are well
79 documented for the DDFT (Spriet et al., 2007; Smith et al., 2008; Spriet and McKnight,
80 2009; Spriet and Zwingenberger, 2009; Gutierrez-Nibeyro et al., 2011). A recent report
81 emphasized the importance of the position of the long axis of the limb perpendicular to the
82 magnetic field also for low-field MRI of the SDFT. Leaning to one side as well as internal or
83 external limb rotation during MR image acquisition in the standing horse may create a 'magic
84 angle' artefact in the SDFT at the level of the pastern that should not be confused with tendon
85 pathology (Fig. 1) (Sherlock and Mair, 2016).

86
87
88
89
90
91
92
93
94
95
96
97
98
99
100
101
102
103
104
105
106
107
108
109
110

MRI for monitoring of tendon lesions

Since MRI has been established as a sensitive tool for the diagnosis of tendinopathies in the equine patient, the value of repeated MRI for monitoring purposes has been further investigated. Sequential MRI evaluation of DDFT lesions in clinical cases has shown that resolution of STIR-FSE and T2-FSE signal changes over time appear to be positive prognostic indicators, whilst most lesions remain visible on T1-GRE and PD images even in cases with excellent outcome (Holowinski et al., 2010; Vanel et al., 2012). Horses with T1-GRE hyperintense DDFT lesions over 30mm in length or over 10% cross-sectional area, as well as horses with persistent STIR-FSE signal or with concurrent lesions in the foot, are less likely to return to their previous level of exercise (Vanel et al., 2012).

The evolution of different DDFT lesion types varies when assessed over time. Dorsal border lesions showed a more rapid reduction in T2*-GRE volume and ratiometric intensity (ratio between lesion and adjacent cortical bone) than parasagittal and core lesions in clinical cases that were followed over a 6-month period (Milner et al., 2012). No correlation between lameness and lesion signal intensity was found in this study, but long-term telephone follow-up (18 months) of a larger group of horses confirmed that dorsal border lesions seem to have a favourable prognosis for return to some level of activity (73%) when compared to other lesion types (core lesions 41%; parasagittal splits 50%) (Cillan-Garcia et al., 2013). However, overall only approximately 25% of these horses returned to their previous level of exercise. The study additionally showed an effect of lesion location with a worse prognosis identified for insertional or suprasesamoidean lesions of the DDFT when compared to lesions at the level of the navicular bone. Lesions affecting both lobes of the DDFT were not necessarily associated with a worse prognosis than uniaxial defects (Cillan-Garcia et al., 2013).

111
112
113
114
115
116
117
118
119
120
121
122
123
124
125
126
127
128
129
130
131
132
133
134
135

Ultrasonography currently remains the most practical imaging modality for the diagnosis and monitoring of SDFT lesions in a clinical setting (Bubeck and Aarsvold, 2018). It is however important to note that the area of maximal cross-sectional injury in experimentally induced SDFT lesions older than 4 weeks appears approximately 18% smaller on ultrasonographic images when compared to standing low-field MRI (Schramme et al., 2010; Karlin et al., 2011). Similar results were found in naturally occurring SDFT lesions and should be taken into consideration when adjusting the exercise program of a horse with SDFT tendinopathy based on ultrasonographic assessment alone (Berner et al., 2016). During sequential MRI examination, SDFT lesions follow a pattern of signal change that differs from the pattern observed in DDFT lesions over time. MR signal decreases earlier in T2-weighted images than in STIR-FSE images in the SDFT (Schramme et al., 2010; Karlin et al., 2011; Berner et al., 2016; Berner, 2017; Berner et al., 2020).

High-field MRI

Most high-field MRI systems with a field strength of 1 Tesla (T) and above are installed in larger referral centres. Examination is usually performed in a closed-bore magnet and requires the horse to be anaesthetised (Lutter et al., 2015). Due to the higher signal-to-noise ratio and corresponding increased image contrast and resolution, the tendon margins are better defined, and subtle lesions appear more conspicuous on high-field MR images when compared to standing low-field MRI (Ghazinoor et al., 2007; Murray et al., 2009). Whilst tendon lesions and adhesions are generally detected on low- and high-field MR images, small focal lesions (≤ 1 mm in diameter) and subtle dorsal fibrillation of the DDFT may be visible on high-field MRI only (Murray et al., 2009).

136 *'Magic angle MRI'*

137 Similar to the appearance on low-field MRI where the B_0 magnetic field is oriented
138 vertically, the 'magic angle' effect at the distal aspect of the DDFT can be recognised mainly
139 on T1-weighted high-field MR images, when the long axis of the tendon is oriented at
140 approximately 55° ($\pm 5-7^\circ$) to the horizontally oriented static magnetic field (Busoni and
141 Snaps, 2002; Spriet and McKnight, 2009; Werpy et al., 2010). The artefact is characterised
142 by a hyperintense signal and can impact on the interpretation of MR images (Erickson et al.,
143 1991; Erickson et al., 1993). Since tendons generally present with little to no signal on MR
144 images, the intentional application of the 'magic angle' effect has been proposed to further
145 investigate the available signal of the tendon structure. The so called 'magic angle MRI'
146 allows sufficient signal to be obtained using the standard pulse sequences of clinical MRI
147 systems (Bydder et al., 2007). Using this technique, an increased T1 relaxation time has been
148 reported in cases of chronic Achilles tendinopathy in humans (Marshall et al., 2002; Oatridge
149 et al., 2003).

150

151 In an initial 'magic angle MRI' study on equine specimens, reference values for the
152 normal T1 relaxation times of the equine SDFT, DDFT and suspensory ligament were
153 determined (Spriet et al., 2011). To further assess possible changes in T1 relaxation
154 associated with tendinopathy, both laser-induced and naturally occurring SDFT lesions were
155 subsequently evaluated (Spriet et al., 2012). All naturally occurring lesions were visible on
156 conventional as well as on 'magic angle' MR images. Based on the histological findings the
157 authors state however, that 'magic angle MRI' might be advantageous for the identification
158 of diffuse changes in tendon composition, that appeared hypointense on conventional MR
159 imaging (Spriet et al., 2012). Whilst the feasibility of 'magic angle MRI' has been

160 demonstrated in high-and low-field MRI systems, the adequate positioning of the limb may
161 still prove to be a challenge in an *in vivo* setting (Spriet et al., 2012; Horstmeier et al., 2019).

162

163 *Influence of local injection on MRI interpretation*

164 Research assessing the influence of diagnostic analgesia on MR image interpretation
165 showed that perineural analgesia of the palmar digital nerves, as well as intra-synovial
166 analgesia of the navicular bursa and the distal interphalangeal joint, do not significantly alter
167 MR images of the distal limb at 1.5 T (Black et al., 2013). Only the injection of 15 ml
168 mepivacaine into the digital flexor tendon sheath caused an iatrogenic increase in synovial
169 fluid volume as detected on MRI at 24 and 72 hours post injection (Black et al., 2013). The
170 study additionally described that needle tracts could not be appreciated consistently at any
171 injection site apart from the site of the navicular bursa injection, where some evidence for a
172 needle tract was detected in 10/15 limbs at 72 hours post injection.

173

174 Another study further investigated the influence of saline injection (30-35 ml) into the
175 digital flexor tendon sheath for the purpose of enhanced ultrasonographic and 1.5 T high-
176 field MR image interpretation (Daniel et al., 2019). The study showed that the presence of
177 fluid significantly improved the delineation of the DDFT in both imaging modalities and the
178 visualisation of the margins of the SDFT on MR images. As the technique did not introduce
179 any artefacts or altered the dimensions of the intra-theal structures, further evaluation in
180 clinical cases should be of value particularly for the detection of marginal tendon lesions. It is
181 however important to consider that patients might be reluctant to stand during low-field MRI
182 following distention of the digital flexor tendon sheath. Consequently, the technique appears
183 to be more suited for high-field MR evaluation.

184

185 In order to facilitate assessment of the dorsal border of the DDFT at the level of the
186 navicular bone, the injection of the navicular bursa with saline (6-10 ml) or a mixture of
187 saline and contrast medium (5-6 ml, 1:1 ratio of 0.9% saline: Diatrizoate Meglumine and
188 Diatrizoate Sodium; Hypaque-76®) has been proposed (Schramme et al., 2009; Maher et al.,
189 2011). The distension of the navicular bursa physically separates the palmar surface of the
190 navicular bone from the dorsal margin of the DDFT and allows adhesions, DDFT fibrillation
191 and tendon splits at this level to be recognized more readily. The limitations of the technique
192 include the time required for the navicular bursa injection under radiographic guidance, and
193 the risk of rupture of the navicular bursa, especially if a volume in excess of 5 ml is injected
194 (Schramme et al., 2009; Maher et al., 2011). Alternatively, the distension of the distal
195 interphalangeal joint with saline (20-35 ml) alters the position of the proximal recess of the
196 navicular bursa and enhances the visualisation of the dorsal border of the DDFT, similar to
197 the direct approach to the navicular bursa (McGill et al., 2015). Both techniques are described
198 to be more reliable in the non-weightbearing limb when no pressure is exerted between the
199 navicular bone and the DDFT and are therefore probably more suitable for high-field MRI *in*
200 *vivo* (Maher et al., 2011; McGill et al., 2015).

201

202 *Contrast-enhanced MRI*

203 Gadolinium-based contrast-enhanced MRI is routinely performed for human and
204 small animal neurologic, oncologic and vascular imaging (Owen, 2018; Scott, 2018).
205 Gadolinium shortens the relaxation time constants (T1 and T2) of the tissues, which leads to
206 an increase in signal intensity, especially in T1-weighted images (Lin and Brown, 2007).
207 First clinical reports recommended an intra-venous gadopentate dimeglumine dose of 0.1
208 ml/kg (50 ml/horse) for musculoskeletal contrast-enhanced MRI in horses (Judy et al., 2008;
209 Saveraid and Judy, 2012; Daniel et al., 2013). The authors described the potential for an

210 improved recognition and assessment of tendon lesions, similar to the human Achilles
211 tendon, where a correlation between contrast enhancement and the severity of tendon lesions
212 has been demonstrated in a number of clinical cases (Shalabi et al., 2002; Richards et al.,
213 2010).

214

215 In order to decrease the volume and associated expense of gadolinium required for
216 contrast-enhanced MRI in horses, regional limb perfusion with gadopentate dimeglumine (5
217 ml in 5 ml 0.9% saline) via the palmar/plantar digital vein at the level of the mid
218 metacarpus/metatarsus was evaluated in a prospective clinical study (Aarsvold et al., 2018).
219 Pre- and post-contrast high-field (1.5 T) MRI was performed in anaesthetized horses in
220 lateral recumbency. Contrast enhancement in the distal limb was adequate provided the
221 tourniquet was secured in place. Multiple lesions were identified and were mostly visible on
222 pre-contrast as well as contrast-enhanced MR images. The authors describe, however, that the
223 technique aids the characterisation of lesions including adhesions and neovascularisation of
224 the DDFT (Aarsvold et al., 2018). In the standing horse the approach may be limited due to
225 difficulties in ensuring patients stand still for the requisite amount of time for the examination
226 post tourniquet application. Additionally, it might be challenging to replicate the exact
227 position of the foot in the magnet pre- and post contrast injection.

228

229 A further study compared systemic intra-venous injection with regional intra-arterial
230 injection of gadolinium in a group of horses with lameness localized to the foot (De Zani et
231 al., 2018). The injection of 0.02 ml/kg of gadolinium in the radial artery resulted in a higher
232 ratio of MRI contrast enhancement when compared to the systemic intra-venous route (0.1
233 ml/kg). Whilst the tendon tissue appeared generally not highly vascularised, significant

234 enhancement of the DDFT and peritendinous tissue was noted in the area of suspected
235 pathological lesions (De Zani et al., 2018).

236

237 The contrast enhancement in association with tendinopathy is most likely related to an
238 increased capillary permeability and diffusion of blood into the interstitial space in the acute
239 stages of the injury. Additionally, neovascularisation and granulation tissue formation are
240 suspected to show increased contrast uptake. However, histological studies of contrast-
241 enhancing lesion in the equine distal limb are currently lacking (Shalabi et al., 2002; Saveraid
242 and Judy, 2012; Nelson et al., 2017).

243

244 Side effects of the administration of gadolinium-based contrast agents are described in
245 human and small animal patients, but no severe adverse reactions were encountered in the
246 aforementioned equine studies (Wible et al., 2001; Grobner and Prischl, 2007; Lin and
247 Brown, 2007; Girard and Leece, 2010; Saveraid and Judy, 2012; Prince et al., 2017; Aarsvold
248 et al., 2018; De Zani et al., 2018). A recent review of the use of contrast media in horses
249 classified the risk associated with the administration of gadolinium generally as low,
250 provided horses do not suffer underlying renal disease or dehydration (Nelson et al., 2017).

251 Future research should further ascertain the benefits of contrast-enhanced over standard MRI
252 for the assessment of tendon lesions and identify how imaging findings correlate with
253 histopathology. Additionally, the combined approach of contrast-enhanced and ‘magic angle
254 MRI’ as described for the human Achilles tendon might be of interest for equine flexor
255 tendon imaging (Marshall et al., 2002).

256

257 **Ultra-high field MRI**

258 The high-field MRI systems currently installed in veterinary centres for clinical
259 applications operate at a field strength of 1.5 to 3 T. Magnets used in humans for clinical
260 purposes have now reached 7 T, and preclinical research ultra-high field MRI systems
261 exceeding a field strength of 10 T are available (Alizai et al., 2018; Ladd et al., 2018).

262

263 Low- and high-field MRI facilitates the detection and assessment of tendon lesions,
264 but the visualisation of the tendon structure remains difficult. The very short transverse
265 relaxation time of normal tendon tissue, with the relatively long echo times used in
266 conventional clinical MRI sequences usually result in the complete decay of tendon signal
267 before it can be sampled (Juras et al., 2012; Guidetti et al., 2018; Juras et al., 2019). With
268 increasing field strength and signal-to-noise ratio, and the use of ultrashort echo time (UTE)
269 and other sequences, MR images of the finer tendon structural components can be obtained
270 (Fig. 2) (Robson et al., 2004; Du et al., 2010; Moser et al., 2012; Juras et al., 2013; Chang et
271 al., 2015; Foure, 2016). In man, ultra-high field MRI is utilized to visualise the fascicular
272 pattern of the Achilles tendon *in vivo* (Han et al., 2014; Foure, 2016; Juras et al., 2019).

273

274 *Ultra-high field MRI of the equine SDFT*

275 Ultra-high field MRI (9.4 T) of the equine SDFT facilitates the detailed assessment of
276 the tendon structure with clear delineation of the tendon fascicles and interfascicular matrix
277 (Fig. 2 A + B). Additionally, T2*-weighted 3D-FISP gradient echo transverse images provide
278 a comprehensive picture for the characterisation of tendon lesions (Fig. 2C). At this stage the
279 size of the radiofrequency coil and the time required to obtain this high level of anatomical
280 detail preclude the *in vivo* assessment of tendon lesions in horses. The cost and technical
281 expertise involved with MR imaging at higher field strength limits its availability in

282 veterinary medicine, however, ultra-high field MRI offers promising prospects for
283 musculoskeletal imaging as clinical progress continues (Alizai et al., 2018; Ladd et al., 2018).

284

285 **Computed tomography**

286 The limited availability of MRI has led to the investigation of alternative modalities
287 for soft tissue advanced diagnostic imaging in equine orthopaedics (Tucker and Sande, 2001;
288 Puchalski, 2012; Jones et al., 2019). A study comparing MRI and CT for the assessment of
289 the equine distal limb found similar scores for the visibility of the DDFT in the area of the
290 pastern for both modalities, but the distal DDFT at the level of insertion showed better
291 visualisation scores with low-field MRI (Vallance et al., 2012a). Likewise, the classification
292 of DDFT lesions varies depending on the imaging modality used for interpretation. More
293 lesions of the distal DDFT were detected with low-field MRI but lesions at the level of the
294 pastern as well as abrasions and mineralisation of the DDFT were more likely to be
295 diagnosed with CT in a cohort of clinical cases (Fig. 3) (Vallance et al., 2012b). Additional
296 reports comparing both, MRI and CT imaging findings of the same subject with results of
297 histopathological examination would give further insight and support image interpretation
298 (Whitton et al., 1998; Puchalski et al., 2009).

299

300 *Contrast-enhanced computed tomography*

301 The contrast media used for CT studies in equine patients are usually iodinated
302 solutions that strongly attenuate X-rays and highlight areas of increased vascular perfusion or
303 permeability (Bushberg et al., 2012; Nelson et al., 2017). Following acquisition of pre-
304 contrast images the intra-vascular or intra-theal route of administration may be chosen for
305 contrast-enhanced CT imaging of the equine distal limb (Puchalski, 2012; Nelson et al.,
306 2017).

307

308 There are some reports of intra-venous contrast studies in the horse (Hunter et al.,
309 2016; Walker et al., 2017). However, the technique most commonly described is the regional
310 intra-arterial injection of contrast medium, including placement of a catheter in the medial
311 palmar artery at the level of the carpometacarpal joint under ultrasonographic guidance in the
312 anaesthetised horse. Steady-state infusion of a 1:1 dilution of ionic-iodinated contrast in
313 saline is subsequently maintained with a remotely controlled pressure injector (2 ml/s),
314 starting 3-5 seconds prior to CT examination (Collins et al., 2004; Puchalski et al., 2005;
315 Puchalski et al., 2007; Puchalski et al., 2009; Pollard and Puchalski, 2011b). Whilst tendon
316 lesions are less common in the hindlimb, contrast application via catheterisation of the lateral
317 dorsal metatarsal artery is also described (van Hamel et al., 2014) (Fig. 4). The normal CT
318 anatomy and attenuation values for tendon and ligament before and after intra-arterial
319 contrast administration have been documented in detail (Tietje et al., 2001; Puchalski et al.,
320 2007; Vallance et al., 2012a; Claerhoudt et al., 2014). The DDFT generally shows a slight but
321 significant increase in post-contrast attenuation (8-17 HU) that potentially impairs on the
322 clear anatomical visualisation of the tendon (Puchalski et al., 2007; Vallance et al., 2012a).

323

324 DDFT lesions in the area of the foot are usually characterised by marked contrast
325 enhancement (> 20 HU) that may be central, peripheral or diffuse (Puchalski et al., 2009;
326 Puchalski, 2011; Vallance et al., 2012b; van Hamel et al., 2014). Lack of contrast
327 enhancement has been occasionally observed in dorsal border lesions of the DDFT. A
328 sensitivity of 93% for lesion detection was determined following histopathological
329 examination of the affected tissue in one study (van Hamel et al., 2014). All false negative
330 results obtained in this study were at the level of the navicular bone where the visibility of the
331 DDFT is most limited on CT images (Vallance et al., 2012a; van Hamel et al., 2014). Clinical

332 studies have shown that lesions of the DDFT can also be diagnosed based on non-contrast-
333 enhanced CT (Tietje et al., 2001; Jones et al., 2019). However, lesions in the area of the
334 DDFT insertion were more likely to be identified post-contrast in one study (Vallance et al.,
335 2012b).

336

337 CT contrast tenography may aid the evaluation of the flexor tendons as they course
338 through the digital flexor tendon sheath (Fig. 5). Consistent delineation of the flexor tendon
339 borders and the *manica flexoria* has been described after intra-theal injection of nonionic-
340 iodinated contrast solution (60 ml) into the digital flexor tendon sheath of cadaver limbs
341 without flexor tendon pathology (Lacitignola et al., 2015; Agass et al., 2018). Further
342 research should confirm the value of this technique for diagnostic purposes and pre-surgical
343 planning.

344

345 Adverse reactions to the intravascular administration of iodinated contrast are rare in
346 horses but may include a transient increase in heart rate and blood pressure as well as local or
347 generalised skin reactions (Gunkel et al., 2004; Pollard and Puchalski, 2011a; Nelson et al.,
348 2017). CT technology is advancing rapidly and the resolution of images obtained for the
349 assessment of clinical cases has considerably increased over the past decade (Puchalski,
350 2012; Riggs, 2018). High slice number multidetector CT scanners are becoming more widely
351 available and first examples of distal limb examination in standing horses have been reported
352 (Desbrosse et al., 2008; Koch et al., 2020; Mageed 2020; Pauwels et al., 2021). In contrast to
353 MR imaging CT does not offer the capability of accurately detecting the fluid content within
354 a tendon lesion to date. However, with its improved image quality and fast acquisition time,
355 CT may provide a practical alternative to MRI for advanced diagnostic imaging of the equine
356 flexor tendons (Riggs, 2018; Jones et al., 2019). Future research should show whether CT

357 imaging is comparable to MRI regarding the assessment of lesion progression over time.
358 Additionally, patient tolerance regarding contrast procedures in the standing horse warrants
359 further investigation.

360

361 *Positron emission tomography*

362 Positron Emission tomography (PET) is a nuclear medicine imaging technique mainly
363 used in the field of human oncology, but orthopaedic applications are also described in man
364 (Fischer et al., 2010; Fischer, 2013; Kim et al., 2015; Eliasson et al., 2016; Aide et al., 2019).
365 In contrast to gamma scintigraphy where planar images are obtained after the injection of a
366 radioactive agent, PET acquires cross-sectional images allowing for three-dimensional
367 assessment of the region of interest (Spriet, 2019). PET is usually combined with CT in order
368 to obtain functional and structural information. As this setup is currently difficult to realise in
369 large patients like horses, a PET scanner used for preclinical brain research has been adapted
370 for PET imaging of the equine distal limb. First reports of PET imaging in equine
371 orthopaedics mainly describe the benefits of the technique for the detection of osseous lesions
372 and enthesopathy (Spriet et al., 2016; Spriet et al., 2018; Spriet et al., 2019; Norvall et al.,
373 2020). PET imaging has been applied for the monitoring of the healing response after
374 Achilles tendon rupture in human patients and increased uptake of the glucose tracer ^{18}F -
375 fluorodeoxyglucose was detected in horses with SDFT and DDFT tendinopathy in one
376 exploratory study (Eliasson et al., 2016; Spriet et al., 2016). Future studies will further
377 determine the value of PET imaging for the assessment of the equine flexor tendons in
378 clinical cases (Spriet, 2019).

379

380 **Conclusion**

381 The rapid and ongoing technological progress and particularly the influence of
382 modern computing has led to the development of a multitude of approaches for soft tissue
383 imaging. Not all techniques described in preclinical studies or human orthopaedic research
384 will be economical or practical enough to be carried through into veterinary clinical
385 diagnostics. However, the last two decades have shown how fast advanced diagnostic
386 imaging modalities including MRI and CT have been integrated in equine orthopaedics at
387 referral level. Both modalities have benefits and disadvantages, particularly for the
388 assessment of flexor tendon injuries. Detailed knowledge of MRI and CT approaches
389 including the implications of the ‘magic angle’ and the use of injection techniques and
390 contrast should aid image interpretation and selection of the appropriate modality. As
391 diagnostic imaging is crucial for the diagnosis and monitoring of equine tendinopathy and
392 potentially aids the prevention of tendon injury, there is ongoing demand for future studies in
393 this developing field of research.

394

395 **Conflict of interest statement**

396 None of the authors has any financial or personal relationships that could
397 inappropriately influence or bias the content of the paper.

398

399 **Acknowledgements**

400 The authors gratefully acknowledge the assistance of Dr. Carolin Müller and Birte
401 Drees (Lucidity Diagnostics) with the preparation of the figures.

402

403 **References:**

404 Aarsvold, S., Solano, M., Garcia-Lopez, J., 2018. Magnetic resonance imaging following
405 regional limb perfusion of gadolinium contrast medium in 26 horses. *Equine*
406 *Veterinary Journal* 50, 649-657.

407

- 408 Agass, R., Dixon, J., Fraser, B., 2018. Computed tomographic contrast tenography of the
409 digital flexor tendon sheath of the equine hindlimb. *Veterinary Radiology &*
410 *Ultrasound* 59, 279-288.
411
- 412 Aide, N., Hicks, R.J., Le Tourneau, C., Lheureux, S., Fanti, S., Lopci, E., 2019. FDG
413 PET/CT for assessing tumour response to immunotherapy : report on the EANM
414 symposium on immune modulation and recent review of the literature. *European*
415 *Journal of Nuclear Medicine and Molecular Imaging* 46, 238-250.
416
- 417 Alizai, H., Chang, G., Regatte, R.R., 2018. MR imaging of the musculoskeletal system using
418 ultrahigh field (7T) MR imaging. *PET Clinics* 13, 551-565.
419
- 420 Arensburg, L., Wilderjans, H., Simon, O., Dewulf, J., Boussauw, B., 2011. Nonseptic
421 tenosynovitis of the digital flexor tendon sheath caused by longitudinal tears in the
422 digital flexor tendons: a retrospective study of 135 tenoscopic procedures. *Equine*
423 *Veterinary Journal* 43, 660-668.
424
- 425 Berner, D., Brehm, W., Gerlach, K., Gittel, C., Offhaus, J., Paebst, F., Scharner, D., Burk, J.,
426 2016. Longitudinal cell tracking and simultaneous monitoring of tissue regeneration
427 after cell treatment of natural tendon disease by low-field magnetic resonance
428 imaging. *Stem Cells International*, 1207190.
429
- 430 Berner, D., 2017. Diagnostic imaging of tendinopathies of the superficial flexor tendon in
431 horses. *The Veterinary Record* 181, 652-654.
432
- 433 Berner, D., Brehm, W., Gerlach, K., Offhaus, J., Scharner, D., Burk, J., 2020. Variation in the
434 MRI signal intensity of naturally occurring equine superficial digital flexor
435 tendinopathies over a 12-month period. *The Veterinary Record* 187, e53.
436
- 437 Black, B., Cribb, N.C., Nykamp, S.G., Thomason, J.J., Trout, D.R., 2013. The effects of
438 perineural and intrasynovial anaesthesia of the equine foot on subsequent magnetic
439 resonance images. *Equine Veterinary Journal* 45, 320-325.
440
- 441 Blunden, A., Dyson, S., Murray, R., Schramme, M., 2006. Histopathology in horses with
442 chronic palmar foot pain and age-matched controls. Part 2: the deep digital flexor
443 tendon. *Equine Veterinary Journal* 38, 23-27.
444
- 445 Blunden, A., Murray, R., Dyson, S., 2009. Lesions of the deep digital flexor tendon in the
446 digit: a correlative MRI and post mortem study in control and lame horses. *Equine*
447 *Veterinary Journal* 41, 25-33.
448
- 449 Bubeck, K.A., Aarsvold, S., 2018. Diagnosis of soft tissue injury in the sport horse.
450 *Veterinary Clinics of North America: Equine Practice* 34, 215-234.
451
- 452 Bushberg, J.T., Seibert, J.A., Leidholdt, E.M., Boone, J.M., 2012. Interaction of radiation
453 with matter. In: *The Essential Physics of Medical Imaging*. Third Edn. Lippincott,
454 Williams & Wilkins, Philadelphia, PA, USA, pp. 33-59.
455

- 456 Busoni, V., Snaps, F., 2002. Effect of deep digital flexor tendon orientation on magnetic
457 resonance imaging signal intensity in isolated equine limbs-the magic angle effect.
458 *Veterinary Radiology & Ultrasound* 43, 428-430.
459
- 460 Bydder, M., Rahal, A., Fullerton, G.D., Bydder, G.M., 2007. The magic angle effect: a source
461 of artifact, determinant of image contrast, and technique for imaging. *Journal of*
462 *Magnetic Resonance Imaging* 25, 290-300.
463
- 464 Chang, E.Y., Du, J., Chung, C.B., 2015. UTE imaging in the musculoskeletal system. *Journal*
465 *of Magnetic Resonance Imaging* 41, 870-883.
466
- 467 Cillan-Garcia, E., Milner, P.I., Talbot, A., Tucker, R., Hendey, F., Boswell, J., Reardon, R.J.,
468 Taylor, S.E., 2013. Deep digital flexor tendon injury within the hoof capsule; does
469 lesion type or location predict prognosis? *The Veterinary Record* 173, 70.
470
- 471 Claerhoudt, S., Bergman, E.H., Saunders, J.H., 2014. Computed tomographic anatomy of the
472 equine foot. *Anatomia Histologia Embryologia* 43, 395-402.
473
- 474 Collins, J.N., Galuppo, L.D., Thomas, H.L., Wisner, E.R., Hornof, W.J., 2004. Use of
475 computed tomography angiography to evaluate the vascular anatomy of the distal
476 portion of the forelimb of horses. *American Journal of Veterinary Research* 65, 1409-
477 1420.
478
- 479 Daniel, A.J., Judy, C.E., Saveraid, T., 2013. Magnetic resonance imaging of the
480 metacarpo(tarso)phalangeal region in clinically lame horses responding to diagnostic
481 analgesia of the palmar nerves at the base of the proximal sesamoid bones: five cases.
482 *Equine Veterinary Education* 25, 222-228.
483
- 484 Daniel, A.J., Leise, B.S., Selberg, K.T., Barrett, M.F., 2019. Enhanced ultrasonographic
485 imaging of the equine distal limb using saline injection of the digital flexor tendon
486 sheath: a cadaver study. *The Veterinary Journal* 247, 26-31.
487
- 488 De Zani, D., Rabbogliatti, V., Ravasio, G., Pettinato, C., Giancamillo, M.D., Zani, D.D.,
489 2018. Contrast enhanced magnetic resonance imaging of the foot in horses using
490 intravenous versus regional intraarterial injection of gadolinium. *Open Veterinary*
491 *Journal* 8, 471-478.
492
- 493 del Junco, C.I., Mair, T.S., Powell, S.E., Milner, P.I., Font, A.F., Schwarz, T., Weaver, M.P.,
494 2012. Magnetic resonance imaging findings of equine solar penetration wounds.
495 *Veterinary Radiology & Ultrasound* 53, 71-75.
496
- 497 Denoix, J.-M., 1994. Diagnostic techniques for identification and documentation of tendon
498 and ligament injuries. *Veterinary Clinics of North America: Equine Practice* 10, 365-
499 407.
500
- 501 Desbrosse, F.G., Vandeweerd, J.M.E.F., Perrin, R.A.R., Clegg, P.D., Launois, M.T.,
502 Brogniez, L., Gehin, S.P., 2008. A technique for computed tomography (CT) of the
503 foot in the standing horse. *Equine Veterinary Education* 20, 93-98.
504

505 Du, J., Chiang, A.J., Chung, C.B., Statum, S., Znamirovski, R., Takahashi, A., Bydder,
506 G.M., 2010. Orientational analysis of the Achilles tendon and entheses using an
507 ultrashort echo time spectroscopic imaging sequence. *Magnetic Resonance Imaging*
508 28, 178-184.

509

510 Dyson, S., Murray, R., 2007. Magnetic resonance imaging evaluation of 264 horses with foot
511 pain: the podotrochlear apparatus, deep digital flexor tendon and collateral ligaments
512 of the distal interphalangeal joint. *Equine Veterinary Journal* 39, 340-343.

513

514 Dyson, S.J., Murray, R., Schramme, M.C., 2005. Lameness associated with foot pain: results
515 of magnetic resonance imaging in 199 horses (January 2001-December 2003) and
516 response to treatment. *Equine Veterinary Journal* 37, 113-121.

517

518 Eliasson, P., Coupe, C., Lonsdale, M., Svensson, R.B., Neergaard, C., Kjaer, M., Friberg,
519 L., Magnusson, S.P., 2016. Ruptured human Achilles tendon has elevated metabolic
520 activity up to 1 year after repair. *European Journal of Nuclear Medicine and*
521 *Molecular Imaging* 43, 1868-1877.

522

523 Erickson, S.J., Cox, I.H., Hyde, J.S., Carrera, G.F., Strandt, J.A., Estkowski, L.D., 1991.
524 Effect of tendon orientation on MR imaging signal intensity: a manifestation of the
525 "magic angle" phenomenon. *Radiology* 181, 389-392.

526

527 Erickson, S.J., Prost, R.W., Timins, M.E., 1993. The "Magic angle" effect: background
528 physics and clinical relevance. *Radiology* 188, 23-25.

529

530 Fischer, D.R., Maquieira, G.J., Espinosa, N., Zanetti, M., Hesselmann, R., Johayem, A.,
531 Hany, T.F., von Schulthess, G.K., Strobel, K., 2010. Therapeutic impact of
532 [(18)F]fluoride positron-emission tomography/computed tomography on patients with
533 unclear foot pain. *Skeletal Radiology* 39, 987-997.

534

535 Fischer, D.R., 2013. Musculoskeletal imaging using fluoride PET. *Seminars in Nuclear*
536 *Medicine* 43, 427-433.

537

538 Foure, A., 2016. New imaging methods for non-invasive assessment of mechanical,
539 structural, and biochemical properties of human Achilles tendon: a mini review.
540 *Frontiers in Physiology* 7, 324.

541

542 Ghazinoor, S., Crues, J.V., 3rd, Crowley, C., 2007. Low-field musculoskeletal MRI. *Journal*
543 *of Magnetic Resonance Imaging* 25, 234-244.

544

545 Girard, N.M., Leece, E.A., 2010. Suspected anaphylactoid reaction following intravenous
546 administration of a gadolinium-based contrast agent in three dogs undergoing
547 magnetic resonance imaging. *Veterinary Anaesthesia and Analgesia* 37, 352-356.

548

549 Grobner, T., Prischl, F.C., 2007. Gadolinium and nephrogenic systemic fibrosis. *Kidney*
550 *International* 72, 260-264.

551

552 Guidetti, M., Zampini, M.A., Gandini, G., Gupta, A., Li, W., Magin, R.L., Wang, V.M.,
553 2018. Diffusion tensor imaging of tendons and ligaments at ultra-high magnetic
554 fields. *Critical Reviews in Biomedical Engineering* 46, 311-339.

555
556 Gunkel, C.I., Valverde, A., Robertson, S.A., Thompson, M.S., Keoughan, C.G., Ferrell, E.A.,
557 2004. Treatment for a severe reaction to intravenous administration of diatrizoate in
558 an anesthetized horse. *Journal of the American Veterinary Medical Association* 224,
559 1143-1146.
560
561 Gutierrez-Nibeyro, S.D., Werpy, N.M., White, N.A., 2nd, McCutcheon, J., Weng, H.Y.,
562 Christopher, J.M., 2011. Standing low-field magnetic resonance imaging appearance
563 of normal collateral ligaments of the equine distal interphalangeal joint. *Veterinary*
564 *Radiology & Ultrasound* 52, 521-533.
565
566 Han, M., Larson, P.E., Liu, J., Krug, R., 2014. Depiction of Achilles tendon microstructure in
567 vivo using high-resolution 3-dimensional ultrashort echo-time magnetic resonance
568 imaging at 7 T. *Investigative Radiology* 49, 339-345.
569
570 Holowinski, M., Judy, C., Saveraid, T., Maranda, L., 2010. Resolution of lesions on STIR
571 images is associated with improved lameness status in horses. *Veterinary Radiology*
572 *& Ultrasound* 51, 479-484.
573
574 Horstmeier, C., Ahrberg, A.B., Berner, D., Burk, J., Gittel, C., Hillmann, A., Offhaus, J.,
575 Brehm, W., 2019. In vivo magic angle magnetic resonance imaging for cell tracking
576 in equine low-field MRI. *Stem Cells International* 2019, 1-9.
577
578 Hunter, B.G., Huber, M.J., Nemanic, S., 2016. The use of computed tomography to diagnose
579 bilateral forelimb tendon pathology in a horse with unilateral lameness. *Equine*
580 *Veterinary Education* 28, 439-443.
581
582 Jones, A.R.E., Ragle, C.A., Mattoon, J.S., Sanz, M.G., 2019. Use of non-contrast-enhanced
583 computed tomography to identify deep digital flexor tendinopathy in horses with
584 lameness: 28 cases (2014-2016). *Journal of the American Veterinary Medical*
585 *Association* 254, 852-858.
586
587 Judy, C.E., Saveraid, R.C., Rodgers, E.H., Rick, M.C., Herthel, D.J., 2008. Characterization
588 of foot lesions using contrast enhanced equine orthopedic magnetic resonance
589 imaging. In: *Proceedings of the 54th Annual Convention of the American Association*
590 *of Equine Practitioners, San Diego, California, USA, 6th-10th December 2008*, p.
591 459.
592
593 Juras, V., Welsch, G., Bar, P., Kronnerwetter, C., Fujita, H., Trattnig, S., 2012. Comparison
594 of 3T and 7T MRI clinical sequences for ankle imaging. *European Journal of*
595 *Radiology* 81, 1846-1850.
596
597 Juras, V., Apprich, S., Szomolanyi, P., Bieri, O., Deligianni, X., Trattnig, S., 2013. Bi-
598 exponential T2 analysis of healthy and diseased Achilles tendons: an in vivo
599 preliminary magnetic resonance study and correlation with clinical score. *European*
600 *Radiology* 23, 2814-2822.
601
602 Juras, V., Mlynarik, V., Szomolanyi, P., Valkovic, L., Trattnig, S., 2019. Magnetic resonance
603 imaging of the musculoskeletal system at 7T: morphological imaging and beyond.
604 *Topics in Magnetic Resonance Imaging* 28, 125-135.

605
606 Karlin, W.M., Stewart, A.A., Durgam, S.S., Naughton, J.F., O'Dell-Anderson, K.J., Stewart,
607 M.C., 2011. Evaluation of experimentally induced injury to the superficial digital
608 flexor tendon in horses by use of low-field magnetic resonance imaging and
609 ultrasonography. *American Journal of Veterinary Research* 72, 791-798.
610
611 Kasashima, Y., Kuwano, A., Katayama, Y., Taura, Y., Yoshihara, T., 2002. Magnetic
612 resonance imaging application to live horse for diagnosis of tendinitis. *Journal of*
613 *Veterinary Medical Science* 64, 577-582.
614
615 Kim, J.Y., Choi, Y.Y., Kim, Y.H., Park, S.B., Jeong, M.A., 2015. Role of (18)F-fluoride
616 PET/CT over dual-phase bone scintigraphy in evaluation and management of lesions
617 causing foot and ankle pain. *Annals of Nuclear Medicine* 29, 302-312.
618
619 King, J.N., Zubrod, C.J., Schneider, R.K., Sampson, S.N., Roberts, G., 2013. MRI findings in
620 232 horses with lameness localized to the metacarpo(tarso)phalangeal region and
621 without a radiographic diagnosis. *Veterinary Radiology & Ultrasound* 54, 36-47.
622
623 Koch, C., Pauwels, F.E., Schweizer-Gorgas, D., 2020. Technical set-up and case illustration
624 of orthopaedic cone beam computed tomography in the standing horse. *Equine*
625 *Veterinary Education*, (Epub ahead of print) doi: 10.1111/eve.13290.
626
627 Kotani, H., Taura, Y., Sakai, A., Tsuka, T., Kageyama, Y., Nakaichi, M., 2000. Antemortem
628 evaluation for magnetic resonance imaging of the equine flexor tendon. *Journal of*
629 *Veterinary Medical Science* 62, 81-84.
630
631 Lacitignola, L., De Luca, P., Guarracino, A., Crovace, A., 2015. Computed tomographic
632 tenography of normal equine digital flexor tendon sheath: an ex vivo study.
633 *Veterinary Medicine International* 2015, 903169.
634
635 Ladd, M.E., Bachert, P., Meyerspeer, M., Moser, E., Nagel, A.M., Norris, D.G., Schmitter,
636 S., Speck, O., Straub, S., Zaiss, M., 2018. Pros and cons of ultra-high-field MRI/MRS
637 for human application. *Progress in Nuclear Magnetic Resonance Spectroscopy* 109, 1-
638 50.
639
640 Lam, K.H., Parkin, T.D.H., Riggs, C.M., Morgan, K.L., 2007. Descriptive analysis of
641 retirement of Thoroughbred racehorses due to tendon injuries at the Hong Kong
642 Jockey Club (1992-2004). *Equine Veterinary Journal* 39, 143-148.
643
644 Li, T., Mirowitz, S.A., 2003. Manifestation of magic angle phenomenon: comparative study
645 on effects of varying echo time and tendon orientation among various MR sequences.
646 *Magnetic Resonance Imaging* 21, 741-744.
647
648 Lin, S.P., Brown, J.J., 2007. MR contrast agents: physical and pharmacologic basics. *Journal*
649 *of Magnetic Resonance Imaging* 25, 884-899.
650
651 Lutter, J.D., Schneider, R.K., Sampson, S.N., Cary, J.A., Roberts, G.D., Vahl, C.I., 2015.
652 Medical treatment of horses with deep digital flexor tendon injuries diagnosed with
653 high-field-strength magnetic resonance imaging: 118 cases (2000–2010). *Journal of*
654 *the American Veterinary Medical Association* 247, 1309-1318.

655
656 Mageed, M., 2020. Standing computed tomography of the equine limb using a multi-slice
657 helical scanner: Technique and feasibility study. *Equine Veterinary Education*, (Epub
658 ahead of print) doi: 10.1111/eve.13388
659
660 Maher, M.C., Werpy, N.M., Goodrich, L.R., McIlwraith, C.W., 2011. Positive contrast
661 magnetic resonance bursography for assessment of the navicular bursa and
662 surrounding soft tissues. *Veterinary Radiology & Ultrasound* 52, 385-393.
663
664 Mair, T.S., Kinns, J., 2005. Deep digital flexor tendonitis in the equine foot diagnosed by
665 low-field magnetic resonance imaging in the standing patient: 18 cases. *Veterinary
666 Radiology & Ultrasound* 46, 458-466.
667
668 Marshall, H., Howarth, C., Larkman, D.J., Herlihy, A.H., Oatridge, A., Bydder, G.M., 2002.
669 Contrast-enhanced magic-angle MR imaging of the Achilles tendon. *American
670 Journal of Roentgenology* 179, 187-192.
671
672 McGill, S.L., Gutierrez-Nibeyro, S.D., Schaeffer, D.J., Hartman, S.K., O'Brien, R.T., Joslyn,
673 S.K., 2015. Saline arthrography of the distal interphalangeal joint for low-field
674 magnetic resonance imaging of the equine podotrochlear bursa: feasibility study.
675 *Veterinary Radiology & Ultrasound* 56, 417-424.
676
677 Meehan, L., 2017. Should I use magnetic resonance imaging to evaluate horses with foot
678 penetrations? *Equine Veterinary Education* 29, 521-522.
679
680 Milner, P.I., Sidwell, S., Talbot, A.M., Clegg, P.D., 2012. Short-term temporal alterations in
681 magnetic resonance signal occur in primary lesions identified in the deep digital
682 flexor tendon of the equine digit. *Equine Veterinary Journal* 44, 157-162.
683
684 Moser, E., Stahlberg, F., Ladd, M.E., Trattinig, S., 2012. 7-T MR-from research to clinical
685 applications? *NMR in Biomedicine* 25, 695-716.
686
687 Murray, R.C., Roberts, B.L., Schramme, M.C., Dyson, S.J., Branch, M., 2004. Quantitative
688 evaluation of equine deep digital flexor tendon morphology using magnetic resonance
689 imaging. *Veterinary Radiology & Ultrasound* 45, 103-111.
690
691 Murray, R.C., Blunden, T.S., Schramme, M.C., Dyson, S.J., 2006a. How does magnetic
692 resonance imaging represent histologic findings in the equine digit? *Veterinary
693 Radiology & Ultrasound* 47, 17-31.
694
695 Murray, R.C., Schramme, M.C., Dyson, S.J., Branch, M.V., Blunden, T.S., 2006b. Magnetic
696 resonance imaging characteristics of the foot in horses with palmar foot pain and
697 control horses. *Veterinary Radiology & Ultrasound* 47, 1-16.
698
699 Murray, R.C., Mair, T.S., Sherlock, C.E., Blunden, A.S., 2009. Comparison of high-field and
700 low-field magnetic resonance images of cadaver limbs of horses. *The Veterinary
701 Record* 165, 281-288.
702

- 703 Nelson, B.B., Goodrich, L.R., Barrett, M.F., Grinstaff, M.W., Kawcak, C.E., 2017. Use of
704 contrast media in computed tomography and magnetic resonance imaging in horses:
705 techniques, adverse events and opportunities. *Equine Veterinary Journal* 49, 410-424.
706
- 707 Norvall, A., Spriet, M., Espinosa, P., Arino-Estrada, G., Murphy, B.G., Katzman, S.A.,
708 Galuppo, L.D., 2020. Chondrosesamoidean ligament enthesopathy: prevalence and
709 findings in a population of lame horses imaged with positron emission tomography.
710 *Equine Veterinary Journal*, (Epub ahead of print) doi: 10.1111/evj.13299.
711
- 712 O'Callaghan, M.W., 1991. Future diagnostic methods. A brief look at new technologies and
713 their potential application to equine diagnosis. *Veterinary Clinics of North America:
714 Equine Practice* 7, 467-479.
715
- 716 Oatridge, A., Herlihy, A., Thomas, R.W., Wallace, A.L., Puri, B.K., Larkman, D.J., Bydder,
717 G.M., 2003. Magic angle imaging of the Achilles tendon in patients with chronic
718 tendonopathy. *Clinical Radiology* 58, 384-388.
719
- 720 Owen, M., 2018. Radiographic, computed tomography, and magnetic resonance contrast
721 media. In: *Textbook of Veterinary Diagnostic Radiology*. Seventh Edn. Elsevier
722 Saunders, St. Louis, MO, USA, pp. 96-109.
723
- 724 Park, R.D., Nelson, T.R., Hoopes, P.J., 1987. Magnetic resonance imaging of the normal
725 equine digit and metacarpophalangeal joint. *Veterinary Radiology* 28, 105-116.
726
- 727 Pauwels, F.E., Van der Vekens, E., Christan, Y., Koch, C., Schweizer, D., 2021. Feasibility,
728 indications, and radiographically confirmed diagnoses of standing extremity cone
729 beam computed tomography in the horse. *Veterinary Surgery* 50, 365-374.
730
- 731 Peh, W.C.G., Chan, J.H.M., 1998. The magic angle phenomenon in tendons: effect of
732 varying the MR echo time. *British Journal of Radiology* 71, 31-36.
733
- 734 Pollard, R., Puchalski, S., 2011a. CT contrast media and applications. In: *Veterinary
735 Computed Tomography*. First Edn. Wiley Blackwell, Sussex, UK, pp. 57-65.
736
- 737 Pollard, R.E., Puchalski, S.M., 2011b. Reaction to intraarterial ionic iodinated contrast
738 medium administration in anesthetized horses. *Veterinary Radiology & Ultrasound*
739 52, 441-443.
740
- 741 Prince, M.R., Lee, H.G., Lee, C.H., Youn, S.W., Lee, I.H., Yoon, W., Yang, B., Wang, H.,
742 Wang, J., Shih, T.T., et al., 2017. Safety of gadobutrol in over 23,000 patients: the
743 GARDIAN study, a global multicentre, prospective, non-interventional study.
744 *European Radiology* 27, 286-295.
745
- 746 Puchalski, S.M., Snyder, J.R., Hornof, W.J., Macdonald, M.H., Galuppo, L.D., 2005.
747 Contrast-enhanced computed tomography of the equine distal extremity. In:
748 *Proceedings of the 51th Annual Convention of the American Association of Equine
749 Practitioners*, Seattle, Washington, USA, 3rd-7th December 2005, pp. 389-394.
750

- 751 Puchalski, S.M., Galuppo, L.D., Hornof, W.J., Wisner, E.R., 2007. Intraarterial contrast-
752 enhanced computed tomography of the equine distal extremity. *Veterinary Radiology*
753 & *Ultrasound* 48, 21-29.
754
- 755 Puchalski, S.M., Galuppo, L.D., Drew, C.P., Wisner, E.R., 2009. Use of contrast-enhanced
756 computed tomography to assess angiogenesis in deep digital flexor tendonopathy in a
757 horse. *Veterinary Radiology & Ultrasound* 50, 292-297.
758
- 759 Puchalski, S., 2011. Equine foot. In: *Veterinary Computed Tomography*. First Edn. Wiley
760 Blackwell, Sussex, UK, pp. 463-471.
761
- 762 Puchalski, S.M., 2012. Advances in equine computed tomography and use of contrast media.
763 *Veterinary Clinics of North America: Equine Practice* 28, 563-581.
764
- 765 Richards, P.J., McCall, I.W., Day, C., Belcher, J., Maffulli, N., 2010. Longitudinal
766 microvascularity in Achilles tendinopathy (Power Doppler ultrasound, magnetic
767 resonance imaging time-intensity curves and the Victorian Institute of Sport
768 Assessment-Achilles questionnaire): a pilot study. *Skeletal Radiology* 39, 509-521.
769
- 770 Richardson, M.L., Amini, B., Richards, T.L., 2018. Some new angles on the magic angle:
771 what MSK radiologists know and don't know about this phenomenon. *Skeletal*
772 *Radiology* 47, 1673-1681.
773
- 774 Riggs, C.M., 2018. Computed tomography in equine orthopaedics – the next great leap?
775 *Equine Veterinary Education* 31, 151-153.
776
- 777 Robson, M.D., Benjamin, M., Gishen, P., Bydder, G.M., 2004. Magnetic resonance imaging
778 of the Achilles tendon using ultrashort TE (UTE) pulse sequences. *Clinical Radiology*
779 59, 727-735.
780
- 781 Saveraid, T.C., Judy, C.E., 2012. Use of intravenous gadolinium contrast in equine magnetic
782 resonance imaging. *Veterinary Clinics of North America: Equine Practice* 28, 617-
783 636.
784
- 785 Schiavo, S., Cillan-Garcia, E., Elce, Y., Liuti, T., Taylor, S.E., 2018. Horses with solar foot
786 penetration, deep digital flexor tendon injury, and absence of concurrent synovial
787 sepsis can have a positive outcome. *Veterinary Radiology & Ultrasound* 59, 697-704.
788
- 789 Schramme, M., Kerekes, Z., Hunter, S., Nagy, K., Pease, A., 2009. Improved identification of
790 the palmar fibrocartilage of the navicular bone with saline magnetic resonance
791 bursography. *Veterinary Radiology & Ultrasound* 50, 606-614.
792
- 793 Schramme, M., Kerekes, Z., Hunter, S., Labens, R., 2010. Mr imaging features of surgically
794 induced core lesions in the equine superficial digital flexor tendon. *Veterinary*
795 *Radiology & Ultrasound* 51, 280-287.
796
- 797 Scott, L.J., 2018. Gadobutrol: A review in contrast-enhanced MRI and MRA. *Clinical Drug*
798 *Investigation* 38, 773-784.
799

800 Shalabi, A., Kristoffersen-Wiberg, M., Papadogiannakis, N., Aspelin, P., Movin, T., 2002.
801 Dynamic contrast-enhanced mr imaging and histopathology in chronic Achilles
802 tendinosis. A longitudinal MR study of 15 patients. *Acta Radiologica* 43, 198-206.
803

804 Sherlock, C.E., Mair, T.S., Ireland, J., Blunden, T., 2015. Do low field magnetic resonance
805 imaging abnormalities correlate with macroscopical and histological changes within
806 the equine deep digital flexor tendon? *Research in Veterinary Science* 98, 92-97.
807

808 Sherlock, C.E., Mair, T.S., 2016. Magic angle effect on low field magnetic resonance images
809 in the superficial digital flexor tendon in the equine proximal pastern region. *The
810 Veterinary Journal* 217, 126-131.
811

812 Sherlock, C., Fairburn, A., Lawson, A., Mair, T., 2019. The use of magnetic resonance
813 imaging for the assessment of distal limb wounds in horses: A pilot study. *Equine
814 Veterinary Education* 32, 637-645.
815

816 Smith, M.R., Wright, I.M., Smith, R.K., 2007. Endoscopic assessment and treatment of
817 lesions of the deep digital flexor tendon in the navicular bursae of 20 lame horses.
818 *Equine Veterinary Journal* 39, 18-24.
819

820 Smith, M.A., Dyson, S.J., Murray, R.C., 2008. Is a magic angle effect observed in the
821 collateral ligaments of the distal interphalangeal joint or the oblique sesamoidean
822 ligaments during standing magnetic resonance imaging? *Veterinary Radiology &
823 Ultrasound* 49, 509-515.
824

825 Spriet, M., Mai, W., McKnight, A., 2007. Asymmetric signal intensity in normal collateral
826 ligaments of the distal interphalangeal joint in horses with a low-field MRI system
827 due to the magic angle effect. *Veterinary Radiology & Ultrasound* 48, 95-100.
828

829 Spriet, M., McKnight, A., 2009. Characterization of the magic angle effect in the equine deep
830 digital flexor tendon using a low-field magnetic resonance system. *Veterinary
831 Radiology & Ultrasound* 50, 32-36.
832

833 Spriet, M., Zwingenberger, A., 2009. Influence of the position of the foot on MRI signal in
834 the deep digital flexor tendon and collateral ligaments of the distal interphalangeal
835 joint in the standing horse. *Equine Veterinary Journal* 41, 498-503.
836

837 Spriet, M., Wisner, E.R., Anthenill, L.A., Buonocore, M.H., 2011. Determination of T1
838 relaxation time of normal equine tendons using magic angle magnetic resonance
839 imaging. *Veterinary Radiology & Ultrasound* 52, 149-153.
840

841 Spriet, M., Murphy, B., Vallance, S.A., Vidal, M.A., Whitcomb, M.B., Wisner, E.R., 2012.
842 Magic angle magnetic resonance imaging of diode laser induced and naturally
843 occurring lesions in equine tendons. *Veterinary Radiology & Ultrasound* 53, 394-401.
844

845 Spriet, M., Espinosa, P., Kyme, A.Z., Stepanov, P., Zavarzin, V., Schaeffer, S., Katzman,
846 S.A., Galuppo, L.D., Beylin, D., 2016. Positron emission tomography of the equine
847 distal limb: exploratory study. *Veterinary Radiology & Ultrasound* 57, 630-638.
848

- 849 Spriet, M., Espinosa, P., Kyme, A.Z., Phillips, K.L., Katzman, S.A., Galuppo, L.D.,
850 Stepanov, P., Beylin, D., 2018. ¹⁸F-sodium fluoride positron emission tomography of
851 the equine distal limb: Exploratory study in three horses. *Equine Veterinary Journal*
852 50, 125-132.
- 853
854 Spriet, M., 2019. PETting horses? *Equine Veterinary Journal* 51, 283-284.
- 855
856 Spriet, M., Espinosa-Mur, P., Cissell, D.D., Phillips, K.L., Arino-Estrada, G., Beylin, D.,
857 Stepanov, P., Katzman, S.A., Galuppo, L.D., Garcia-Nolen, T., et al., 2019. ¹⁸F-
858 sodium fluoride positron emission tomography of the racing Thoroughbred fetlock:
859 validation and comparison with other imaging modalities in nine horses. *Equine*
860 *Veterinary Journal* 51, 375-383.
- 861
862 Takahashi, T., Kasashima, Y., Ueno, Y., 2004. Association between race history and risk of
863 superficial digital flexor tendon injury in Thoroughbred racehorses. *Journal of the*
864 *American Veterinary Medical Association* 225, 90-93.
- 865
866 Tietje, S., Nowak, M., Petzoldt, S., Weiler, H., 2001. Computed tomographic evaluation of
867 the distal aspect of the deep digital flexor tendon (DDFT) in horses. *Pferdeheilkunde*
868 17, 21-29.
- 869
870 Tucker, R.L., Sande, R.D., 2001. Computed tomography and magnetic resonance imaging in
871 equine musculoskeletal conditions. *Veterinary Clinics of North America: Equine*
872 *Practice* 17, 145-157.
- 873
874 Vallance, S.A., Bell, R.J., Spriet, M., Kass, P.H., Puchalski, S.M., 2012a. Comparisons of
875 computed tomography, contrast enhanced computed tomography and standing low-
876 field magnetic resonance imaging in horses with lameness localised to the foot. Part
877 1: anatomic visualisation scores. *Equine Veterinary Journal* 44, 51-56.
- 878
879 Vallance, S.A., Bell, R.J., Spriet, M., Kass, P.H., Puchalski, S.M., 2012b. Comparisons of
880 computed tomography, contrast-enhanced computed tomography and standing low-
881 field magnetic resonance imaging in horses with lameness localised to the foot. Part
882 2: Lesion identification. *Equine Veterinary Journal* 44, 149-156.
- 883
884 van Hamel, S.E., Bergman, H.J., Puchalski, S.M., de Groot, M.W., van Weeren, P.R., 2014.
885 Contrast-enhanced computed tomographic evaluation of the deep digital flexor tendon
886 in the equine foot compared to macroscopic and histological findings in 23 limbs.
887 *Equine Veterinary Journal* 46, 300-305.
- 888
889 Vanel, M., Olive, J., Gold, S., Mitchell, R.D., Walker, L., 2012. Clinical significance and
890 prognosis of deep digital flexor tendinopathy assessed over time using MRI.
891 *Veterinary Radiology & Ultrasound* 53, 621-627.
- 892
893 Walker, W.T., Ducharme, N.G., Tran, J., Scrivani, P.V., 2017. Nonselective computed
894 tomography angiography for detecting arterial blood flow to the distal limb following
895 trauma in two small equids. *Equine Veterinary Education* 29, 15-21.
- 896

- 897 Werpy, N.M., Ho, C.P., Kawcak, C.E., 2010. Magic angle effect in normal collateral
898 ligaments of the distal interphalangeal joint in horses imaged with a high-field
899 magnetic resonance imaging system. *Veterinary Radiology & Ultrasound* 51, 2-10.
900
- 901 Whitton, R.C., Buckley, C., Donovan, T., Wales, A.D., Dennis, R., 1998. The diagnosis of
902 lameness associated with distal limb pathology in a horse: a comparison of
903 radiography, computed tomography and magnetic resonance imaging. *The Veterinary*
904 *Journal* 155, 223-229.
905
- 906 Wible, J.H., Galen, K.P., Wojdyla, J.K., 2001. Cardiovascular effects caused by rapid
907 administration of gadoversetamide injection in anesthetized dogs. *Investigative*
908 *Radiology* 36, 292-298.
909

910 **Table 1**

911 Overview of the literature validating magnetic resonance imaging (MRI) in the equine distal
 912 limb for the assessment of the superficial digital flexor tendon (SDFT) and the deep digital
 913 flexor tendon (DDFT).

Low-field MRI	Literature source	Area examined	No of horses
0.2 T	Kasashima et al., 2002	SDFT	6
0.27 T	Murray et al. 2009	SDFT / DDFT	10
0.25 T	Karlin et al., 2011	SDFT	8
0.27 T	Sherlock et al., 2015	DDFT	26
<hr/>			
High-field MRI			
1.5 T	Murray et al., 2004	DDFT (distal)	38
1.5 T	Murray et al., 2006a	DDFT (distal)	32
1.5 T	Murray et al., 2006b	DDFT (distal)	34
1.5 T	Murray et al., 2009	SDFT / DDFT	10
1.5 T	Blunden et al., 2006	DDFT (distal)	32
1.5 T	Blunden et al., 2009	DDFT (distal)	46

914

915 **Figure legends**

916 Fig 1. T1-weighted gradient echo (GRE) FAST transverse low-field (0.27T) magnetic
917 resonance image of the equine distal limb at proximal pastern level (lateral is to the left). (A)
918 Note the increased T2 signal intense ‘magic angle’ artefact at the mid- to lateral aspect of the
919 superficial digital flexor tendon (SDFT) (black arrow) as observed with ‘leaning in’ or lateral
920 rotation of the limb during image acquisition. (B) lesion of the medial lobe of the SDFT
921 (white arrow) (Image courtesy of Birte Drees, Lucidity Diagnostics 2020).

922

923 Fig. 2. T2*-weighted 3D-FISP (fast imaging with steady-state free precession) gradient echo
924 transverse MR images of the superficial digital flexor tendon (lateral is to the left). (A) 3-year
925 old Irish Sports Horse mare without pre-existing orthopaedic condition. (B) 25-year old
926 Thoroughbred mare without a history of orthopaedic disease. Thinning of the interfascicular
927 matrix is evident as a result of ageing. (C) 8-year old Thoroughbred gelding with clinical SDFT
928 tendinopathy.

929

930 Fig. 3. Transverse computed tomographic (CT) images (soft tissue window without contrast)
931 of the deep digital flexor tendon (DDFT) at the level of the lower pastern (lateral is to the
932 left). (A) Longitudinal split of the lateral lobe of the DDFT (white arrow) with moderate
933 distension of the navicular bursa (black arrow). (B) Dorsal border lesion of the DDFT (white
934 arrow) (Images courtesy of Carolin Müller, Lucidity Diagnostics 2020).

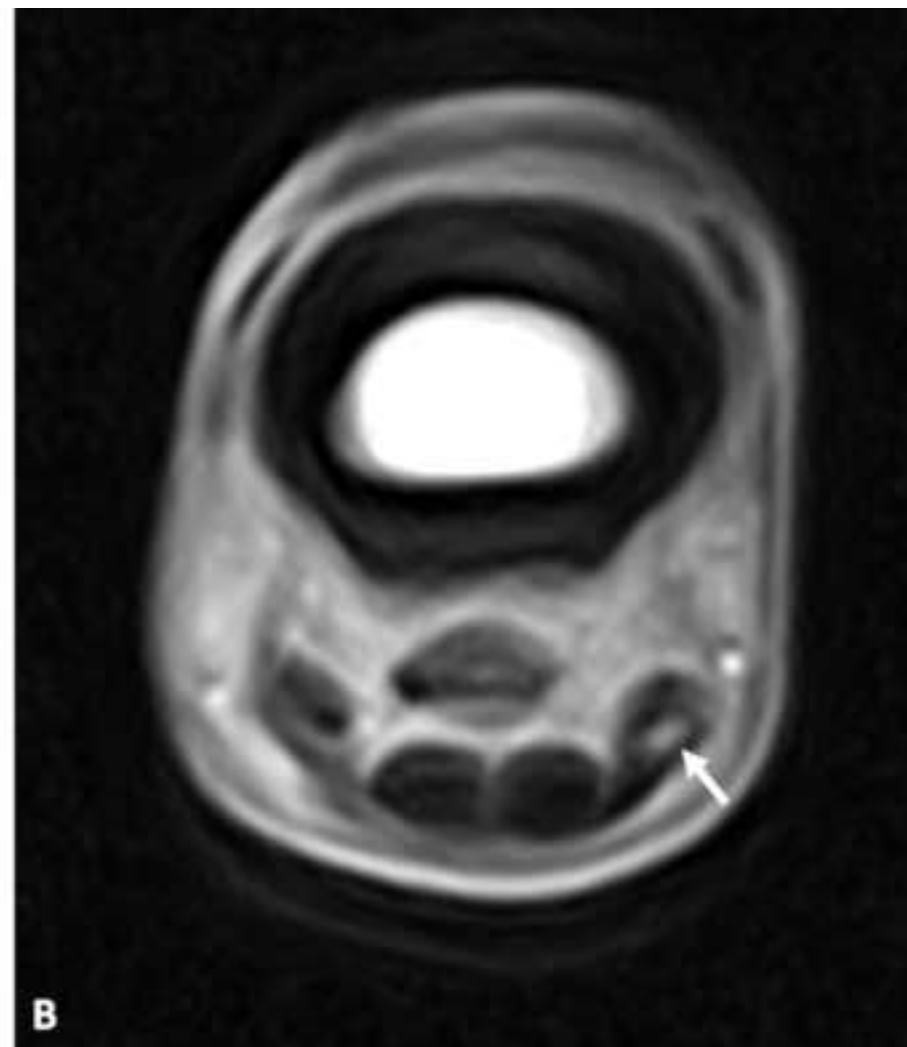
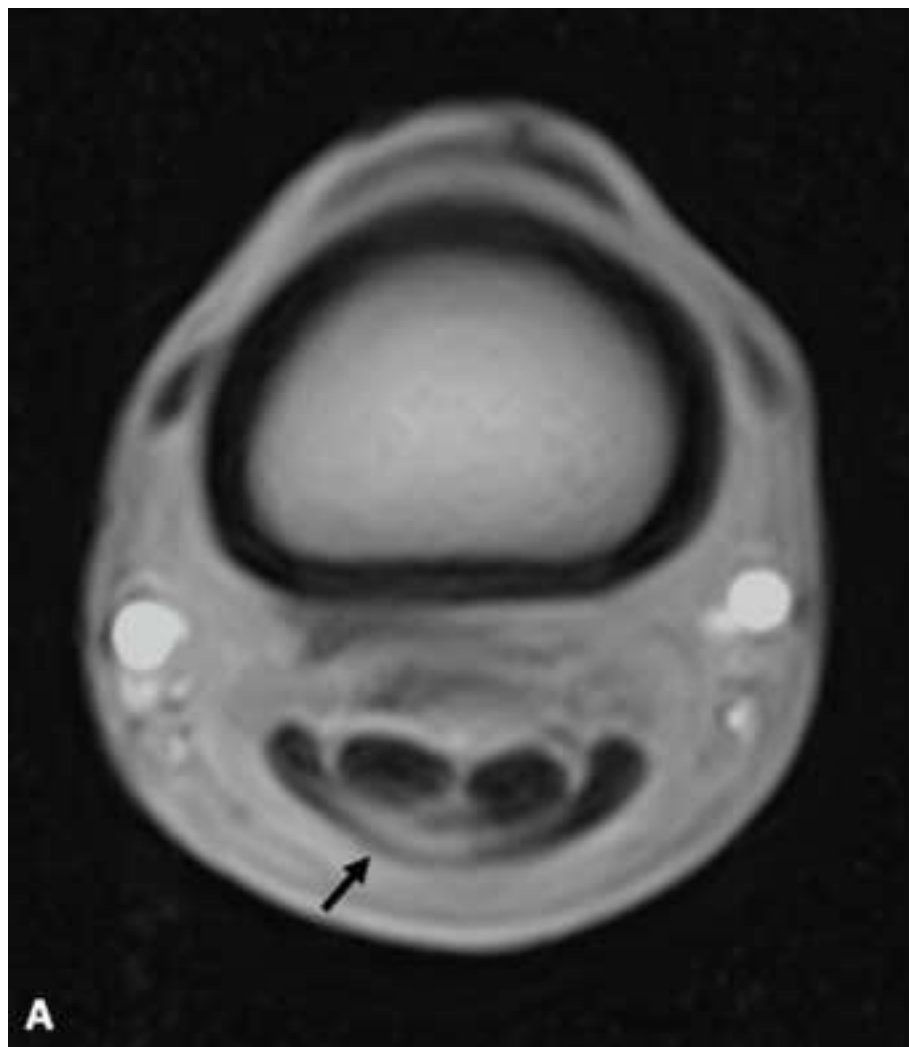
935

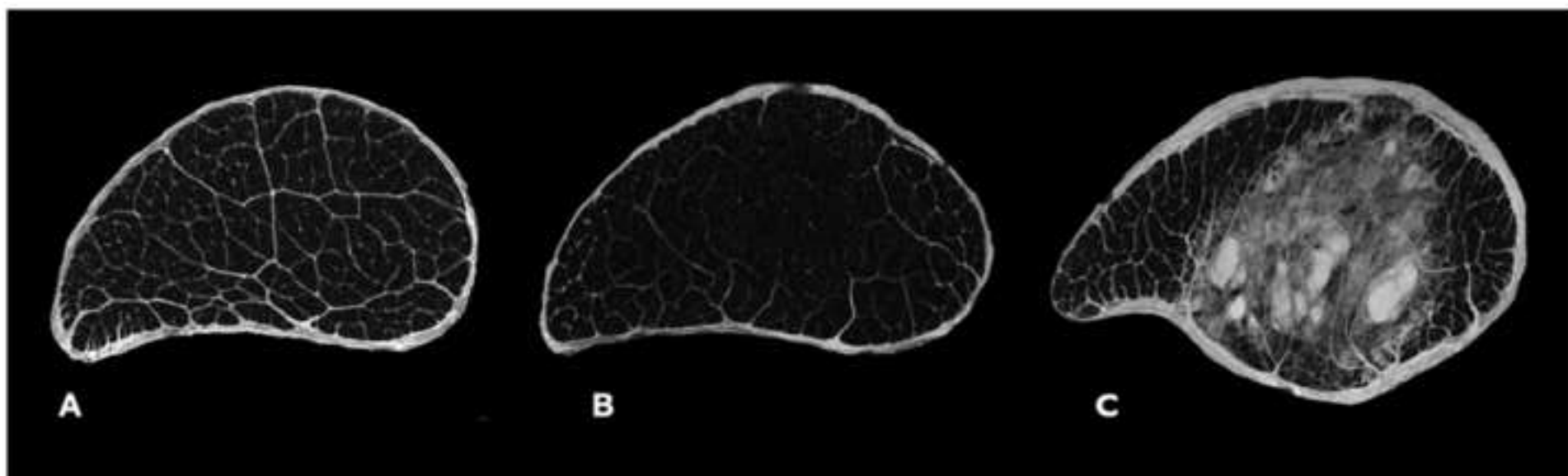
936 Fig. 4. Contrast enhanced computed tomographic images (bone window) showing the deep
937 digital flexor tendon (DDFT) of the left hindlimb of a 10-year-old Warmblood showjumper,
938 acquired during steady-state infusion of ionic-iodinated contrast in saline (1:1; 2ml/s) via the
939 lateral dorsal metatarsal artery (lateral is to the left). (A) Note the increased contrast

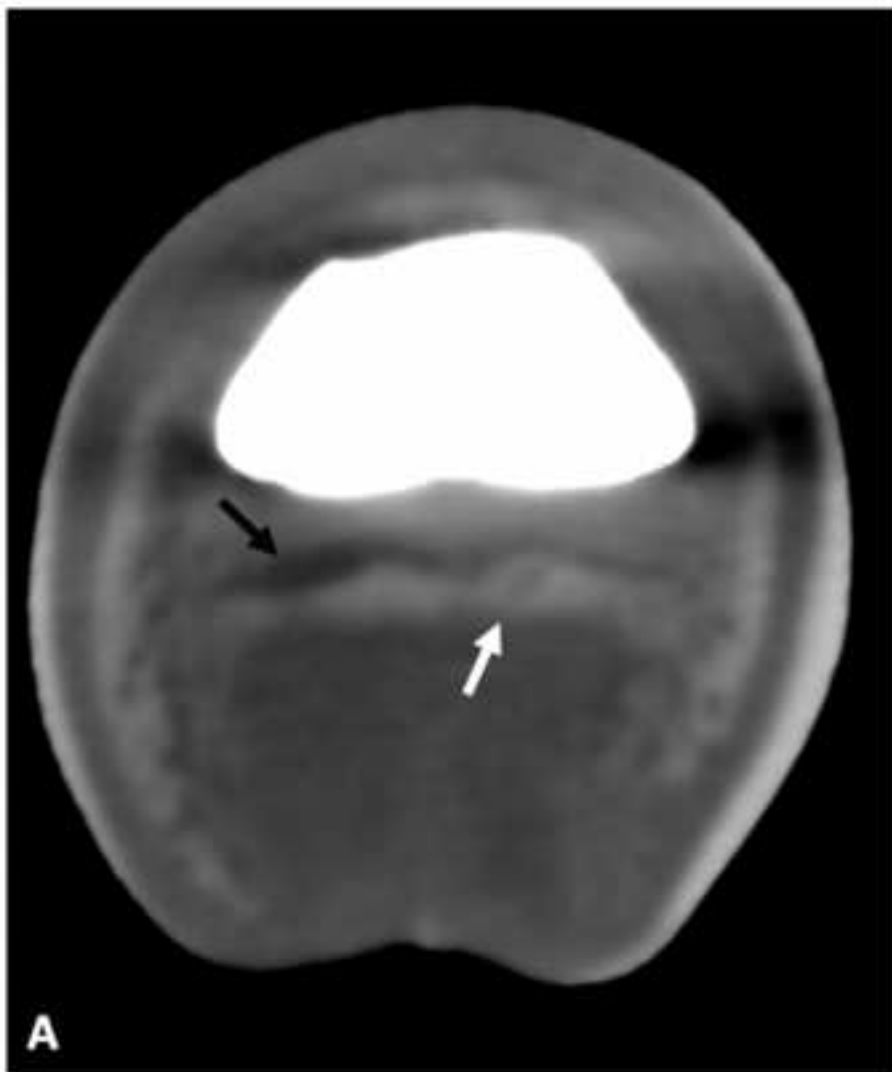
940 enhancement associated with a core lesion of the DDFT in zone 4B (white arrow). (B)
941 Additionally, perilesional contrast attenuation was evident in both lobes of the DDFT in zone
942 P2A (white arrows) in the same horse.

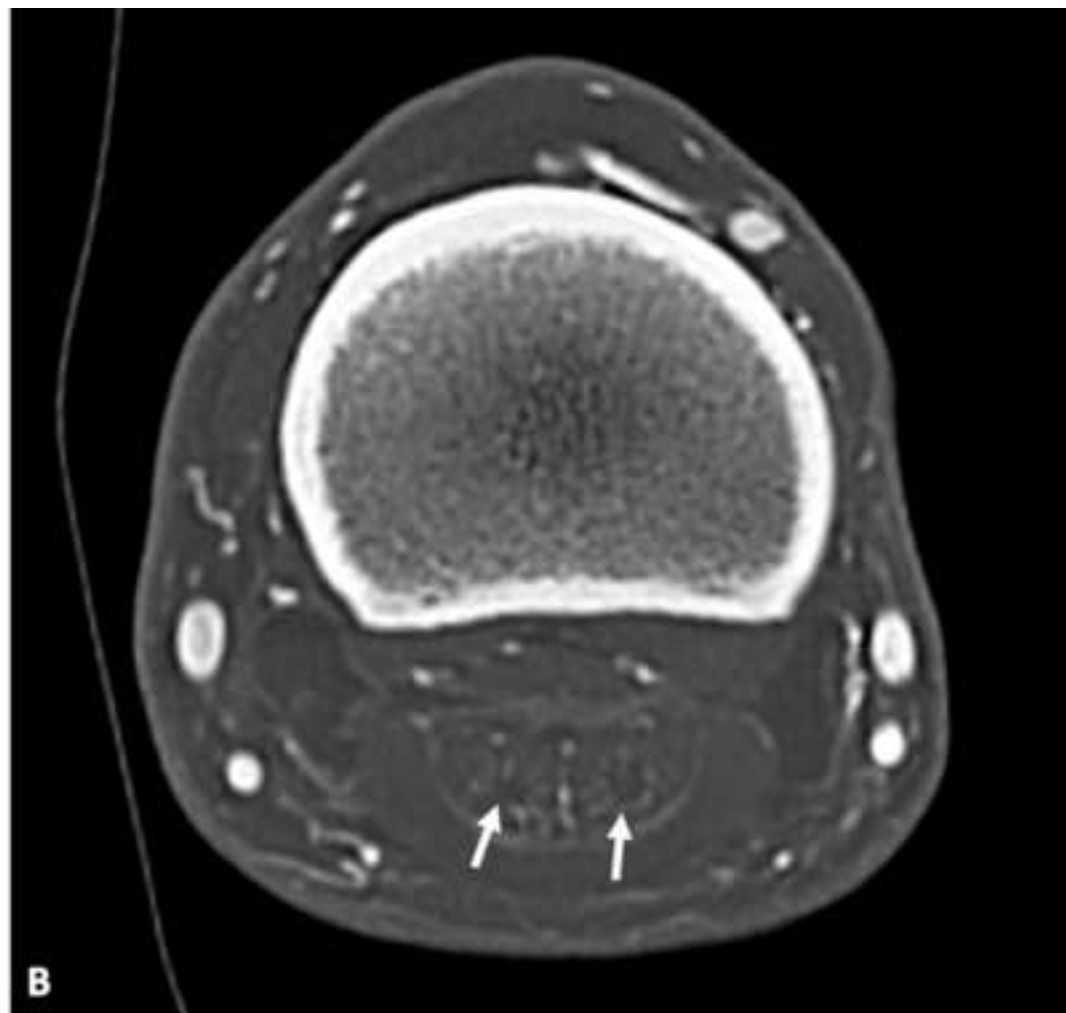
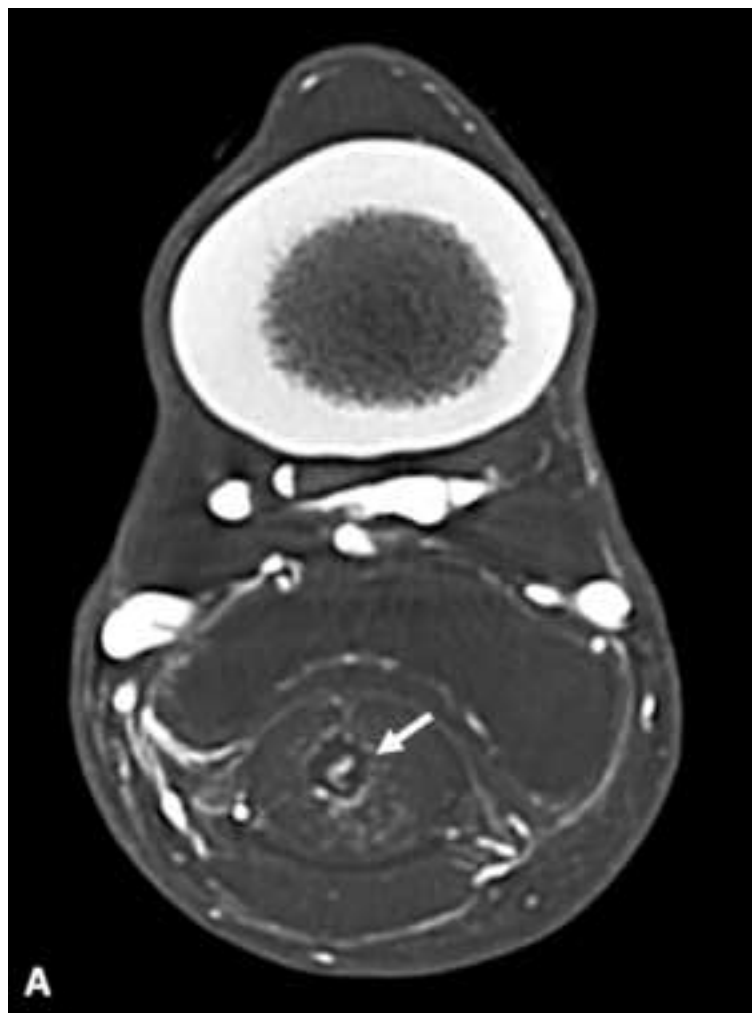
943

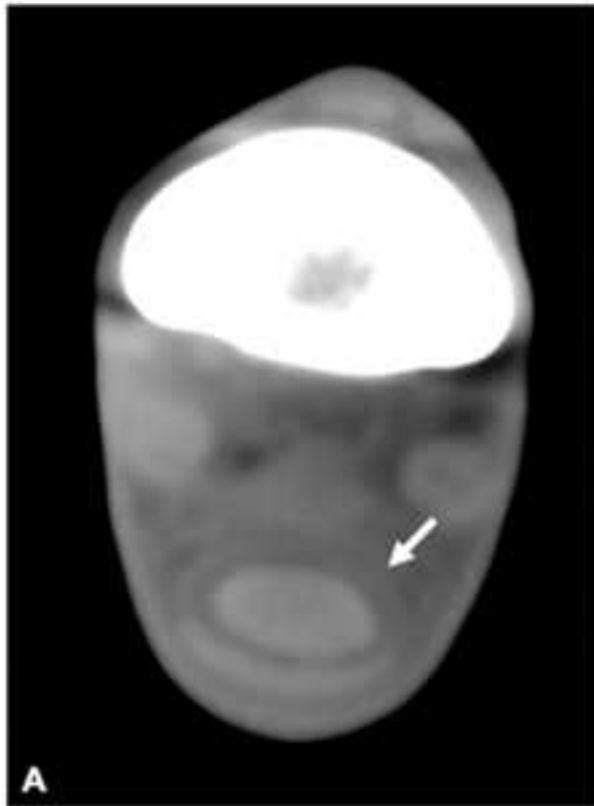
944 Fig. 5. Computed tomographic (CT) images of the flexor tendons at the level of the digital
945 flexor tendon sheath with (B + D) and without (A + C) intra-theal application of nonionic-
946 iodinated contrast. The superficial and deep digital flexor tendons can be recognized on
947 transverse (A) and sagittal (C) CT images using the soft tissue window. The outline of the
948 *manica flexoria* (white arrow) and the flexor tendons is highlighted following injection of the
949 digital flexor tendon sheath with contrast (B + D) (lateral is to the left on Fig. 5 A and B)
950 (Images courtesy of Carolin Müller, Lucidity Diagnostics 2020).











Highlights review part 2 – advanced diagnostic imaging

- The magic angle and the use of contrast may enhance flexor tendon Magnetic Resonance Imaging (MRI)
- Computed tomography finds wider use in equine orthopaedic soft tissue imaging
- Positron emission tomography and ultra-high field MRI provide future prospect is tendon imaging

Revision note – tendon imaging review part 2

The authors would like to thank the reviewers for their valuable comments and suggestions concerning the manuscript ‘Equine flexor tendon imaging part 2 – current status and future directions in advanced diagnostic imaging’.

The manuscript has been revised accordingly and the authors’ response is detailed below.

Changes to the manuscript are highlighted as track changes (reviewing mode). The authors hope that the amended manuscript will satisfy the reviewers concerns and is now considered suitable for publication.

Reviewer #1

Reviewer comment: A very well-written, concise and informative summary of the currently available advanced imaging technology for assessment of tendon pathology. Overall part 2 is written in a slightly more clinically relevant and engaging manner than part 1, with more information regarding the clinical applications of the various technologies and their sensitivity and specificity for lesion detection. I acknowledge that this likely reflects both the authors' experience and the greater wealth of literature available for these modalities. Again, further images would be appreciated, especially in highlighting the utility of contrast enhanced CT in detection of DDFT lesions within the foot as well as examples of lesions of the DDFT and SDFT on low field and high field MRI.

Authors’ response: The authors would like to thank reviewer 1 for the kind words. Additional images were added as requested (Figure 1 + 4).

Reviewer comment: Lines 102-107 - The reported prognoses for lesions in the Cillan-Garcia study are accurate, and reflect return to ridden exercise, however I feel that the authors should make clear that these figures do not reflect the proportion of horses that returned to their previous level of exercise, which were much lower. The effect of lesion location should also be included, as insertional lesions had a worse prognosis than lesions in the region of the navicular bone and navicular bursa.

Authors’ response: The authors agree and have changed the paragraph as requested to state the results of the cited study more accurately (lines126-131).

Reviewer comment: Lines 171-177 - Would it be prudent for the authors to mention that these techniques were performed in high field magnets only, and that the technique would be difficult in standing magnet as patient would likely be reluctant to stand following distention of the sheath?

Authors’ response: In clinical practice the authors frequently perform distention of the digital flexor tendon sheath prior to ultrasonographic evaluation where a mix of radiopaque contrast and local anaesthetic is injected intra-theccally. Contrast radiography and assessment of the block is

subsequently performed, followed by ultrasonographic evaluation. We hardly ever encounter problems with horses that would not stand still for ultrasonographic evaluation with some sedation. However, things might be different in the magnet and we usually do not use more than 25mls in total. The sentence was therefore changed as requested (lines 206-207 and 211-214).

Reviewer comment: Lines 208-216 - again it may be prudent to mention that this approach may be limited in the standing horse due to difficulties in ensuring patients stand still for the requisite amount of time for the examination post tourniquet application as well as difficulties in replicating the positioning of the foot pre and post contrast injection.

Authors' response: The authors would like to thank Reviewer 1 for this valid and practical consideration. The paragraph was changed accordingly (lines 251-252 and 256-259).

Reviewer comment: Lines 297-301 - The approach described is for the forelimb only. Although DDFT lesions are less common in the hindlimb, they are documented to occur. Would it be feasible to add details for intra-arterial contrast in the HL also?

Authors' response: Details about intra-arterial contrast CT in the hindlimb were added to the paragraph (lines 349-351 and Figure 4).

Reviewer comment: Additionally, it is not clear from the manuscript that the recommended protocol would be to acquire pre-contrast images followed by contrast enhanced images on CT. It may be useful to the reader to add a line detailing this.

Authors' response: It is now pointed out in the manuscript that contrast enhanced CT is performed following acquisition of pre-contrast images (lines 336-337).

Reviewer comment: Lines 338-340 - Whilst I agree that the advantages in acquisition time and image resolution due to the availability of thinner slices and reconstructions in different algorithms make CT an attractive prospect for tendon imaging, the additional information on fluid content of tendon lesions on MRI images should not be overlooked. Insufficient work has been performed looking at the progression of lesions over time on CT imaging when compared to MRI. Similarly there is little work looking at the use of contrast procedures in the standing systems. It is my suspicion that intra-arterial contrast may be poorly tolerated in the standing sedated patient.

Authors' response: The authors agree with the mentioned concerns of Reviewer 1 and the paragraph was adjust as requested (lines 386-395).

Reviewer comment: From a practice management/business perspective, the rise in popularity of standing MRI systems has in part been due to the business model of the manufacturer making

these systems affordable with minimal capital outlay (compared with outright purchase of a unit). Additionally, the ability to image under standing sedation and thus avoiding the risks inherent with general anaesthesia has been key to the acceptance of this imaging modality within the horse-owning community. Unless similar business models were to be put in place for standing CT units it is difficult to imagine a similar rapid growth in popularity and availability.

Authors' response: The authors appreciate the reviewer's thought and also believe that it will take years for CT imaging to become as established as MRI for the assessment of orthopaedic conditions in horses. Business models similar to that of Hallmarq where standing examination of the distal limb is possible and the CT unit does not need to be purchased in total are however on the market and appear to be selling well (example Qalibra (Vet-DICon) so far mainly in Europe, UK, Australia and the US, Mageed EVE 2020, line 386).

Mageed, M., 2020. Standing computed tomography of the equine limb using a multi-slice helical scanner: Technique and feasibility study. Equine Veterinary Education, (Epub ahead of print) doi: 10.1111/eve.13388

Reviewer #2:

Reviewer comment: *This manuscript is an accurate representation of a large body of literature assessing advanced imaging of equine tendon. This is a useful review and the authors should be commended for the amount of work put in this manuscript.*

I only have one specific comment, regarding a correction needed in the description of the magic angle effect.

L.68-69: "increased T2 signal". This statement regarding the magic angle effect is misleading. The magic angle effect leads to an increase of the T2 relaxation time, which results in increase signal intensity in sequences with short Echo Time (TE), ie T1 weighted and PD sequences (As mentioned L.73-74). Typically, the magic angle effect is not apparent on T2 weighted sequences, which is an important fact to help distinguish between the artifact and an actual lesion.

Authors' response: The authors would like to thank reviewer 2 for the kind words and for the correction. The sentences were adjusted accordingly (lines 83 and 86-87).

Reviewer #3:

Reviewer comment: *There are two papers titled Parts 1 and 2 but they don't really hang together, because one focuses on the metacarpal region and the other (this one) focuses on the DDFT and the digit. They should be completely separate and the title of this paper should more accurately reflect its content.*

I expected to find information relevant to the SDFT and while this is mentioned in passing, the paper focusses on the DDFT.

Authors' response: The authors appreciate the reviewers concern, and the title of both parts was adjusted to address the issue and state the content of the manuscripts more precisely (lines 3-4).

Reviewer comment: *'Besides lesion detection, future developments in tendon imaging focus on gaining enhanced structural and functional information about the tendon architecture with the prospect to prevent injury.'* - Have you really presented any information to support this statement?

Authors' response: The authors agree, review part one is more focused on the functional assessment and review part two more on structural information. The sentence in the abstract was altered accordingly (lines 28-30).

Reviewer comment: *Line 34 tendon repeats a word in the Title; key words aim to provide additional words for a search engine.*

Authors' response: The keyword 'Tendon' was replaced with 'Tendinopathy' (line 34).

Reviewer comment: The Introduction implies that magic angle MRI is a useful technique whereas the magic angle effect is a term used to describe annoying artefacts which hinder interpretation, as illustrated in Figure 1. I know of no-one using this technique to enhance diagnosis in the equine field, although there are some theoretical ideas about it. I think the method of searching the literature needs to be described without reliance on the other paper.

Authors' response: The statement about the 'magic angle' in the abstract was altered to ensure that it does not imply any information considering the usefulness of 'magic angle' MRI (lines 27-28). Additional details regarding the literature search were added to the introduction (lines 56-59).

Reviewer comment: *Line 41 podotrochlear apparatus would be better terminology than navicular apparatus.*

I would suggest that 'and palmar foot pain' is redundant.

Authors' response: The authors agree and the sentence was altered as requested (line 46).

Reviewer comment: *Line 55 I don't think that you can say that low-field MRI is the gold standard; high field MRI is infinitely superior.*

Authors' response: The authors agree and the sentence was altered accordingly (line 63).

Reviewer comment: The initial validation comparing histology and MRI was done using high-field MRI.

Line 58 1 Tesla is not low-field!

Authors' response: The heading of the paragraph was adjusted to indicate that it is meant to be a more general introduction to MR imaging (line 61). It is indicated in lines 72-74 that the initial validation was performed using high-field MRI.

Reviewer comment: Please make sure that you separate which references relate to low-field and which to high-field and that the reader gets an idea of the numbers of horses and the areas examined in the studies cited - perhaps in Table form.

Authors' response: A table including the requested details was added (Table 1).

Reviewer comment: Part 1 focussed on the metacarpal region - I am curious why this review is extended not only to the DDFT in the hoof capsule, but also those injuries sustained as the result of penetrating injuries.

The use of ultrasonography in the assessment of these lesions has not been discussed. In a 2-part paper of this type I would expect the general anatomical areas under review to be largely the same.

There are numerous references available that discuss the uses and limitations of ultrasonography for evaluation of structures in the digit. This review does not appear to be balanced in its coverage.

Authors' response: The authors agree, review part 1 and part 2 are not balanced regarding the anatomical region discussed. A systematic review assessing the recent literature about flexor tendon imaging was performed without specific focus on the SDFT or the DDFT or the respective level/anatomic region of the tendon within the limb. It is however not a surprise that there is more literature available describing ultrasonographic techniques for the SDFT in the metacarpal region, and for advanced diagnostic imaging techniques of the DDFT at the level of the foot. The tendon each manuscript is focused on is therefore now stated in the title of both parts of the review to prevent confusion.

The literature describing ultrasonographic techniques for the assessment of the DDFT within the foot is particularly valuable for cases where advanced diagnostic imaging is not available or there are financial constraints. The authors however feel that ultrasonography of the foot is not exactly a future trend in equine flexor tendon imaging, and it was therefore not in the focus of the current investigation.

Depending on their exact location, foot penetrations can lead to severe injury of the DDFT and associated structures and the advantages of MRI for their diagnosis is a recent development. Whilst the authors agree that this information goes slightly beyond the scope of the review, we decided to mention the literature describing MR imaging of this particular aspect as it is considered to provide relevant and practical information for the reader and indicates a useful applications of MR imaging.

Reviewer comment: Lines 68-8 What is meant by T2 signal?

You go on to say that the MAE is seen in TIW images

This review is supposed to be about flexor tendon injuries so why are you talking about CL injuries of the DIP joint. Please stick to the subject! MAE is not a big problem with the flexor tendons. Put this into proper perspective. This whole section seems to reflect a lack of understanding of the MAE.

Authors' response: The authors apologise for the use of confusing terminology. The artefact is characterised by increased T2 relaxation time and this has been corrected (line 83). The information concerning the collateral ligaments of the distal interphalangeal joint was removed from the sentence (line 90).

Reviewer comment: Lines 86-95 I do not think that this section represents an accurate overview of the literature. Check which studies actually are longitudinal studies - not all of them are!

Authors' response: The studies that did not include repeated MRI examination were removed from the paragraph (line 118).

Reviewer comment: Line 97 The term 'development' is not appropriate here - I think you are referring to the evolution of lesions over time after diagnosis.

Authors' response: The term 'evolution' was included (line 120).

Reviewer comment: Lines 100 -107 This discussion about prognosis for different types of lesions is not relevant to the paper's title.

Authors' response: As additional detail about the discussion of lesion types was requested, this section was altered as suggested by reviewer 1. The authors would like to defer to the editor to decide how much information should be included here (lines 123-132).

Reviewer comment: Lines 110 - 121 Please be careful to make it absolutely clear whether you are describing the evolution of naturally occurring lesions versus experimentally -induced lesions - they are not the same!

Authors' response: Information regarding the type of lesion was included (lines 143-145).

Reviewer comment: Line 123 Now you say that 1 tesla is high-field!

Authors' response: The authors agree and the introduction of the MRI section was changed to be more precise (line 72).

Reviewer comment: Lines 161-4 reference required

Authors' response: The reference was added (line 198).

Reviewer comment: I think that you need to put into perspective the cost benefit ratio and time benefit ratio of the variety of injection techniques described and think about what is practical and what is in reality being done in practice. Many of these techniques were described > 10 years ago but have not been universally embraced. Moreover the safety aspects and hassle factor (taking limbs in and out of a magnet) must also be considered.

Authors' response: The authors agree and the practical implications of the injection techniques, particularly when considered to be used during low-field MRI were added (also requested by reviewer 1) (lines 211-214).

Reviewer comment: Gadolinium - so do you conclude that with our current knowledge the extra costs and time involved are justified with respect to acquisition of knowledge that is going to influence patient management? I think that a review of this type has to be critical - rather than just describe what has been published - what is of practical value for patient management?

Authors' response: Similar to the previous paragraph, practical considerations were added to this section (lines 251-252). The value of contrast MRI is additionally critically appraised in lines 254-256; 256-259; 273-275.

Reviewer comment: Reviewer comment: Line 252- 264 In part 1 you described focussing on equine literature! Line 264 - is 9T imaging ever going to be affordable for equine practice? Fig. 2 provides some beautiful images but they don't really tell us how they might potentially give us additional useful clinical information over and above ultrasonography. This seems to be another example of how this paper does not really relate enough to what can be usefully used clinically in the real world. Just because something can be done does not mean it should be done unless there is benefit to the clinician and patient. The section on CT and contrast-enhanced CT is the best section of this paper.

Authors' response: The authors appreciate the reviewers concern and agree that some imaging techniques detailed throughout the review might not be practical or valuable enough to become widely accepted in the future. The aim of the review is to give the reader an idea of what research is focused on and what might be possible in the future. The role of the interfascicular matrix in the pathogenesis of tendinopathy has been investigated in detail in recent years and is thought to have major implications in the development of clinically relevant tendon injury (Thorpe et al. 2012/2013). To the author's knowledge ultra-high field MRI is the only imaging technique that facilitates visualisation of the interfascicular matrix

to date. Whilst ultra-high field MRI is far from being introduced in equine practice, the field of diagnostic imaging is advancing rapidly in human as well as veterinary patients.

Thorpe, C.T., Udeze, C.P., Birch, H.L., Clegg, P.D., Screen, H.R.C., 2012. Specialization of tendon mechanical properties results from interfascicular differences. *Journal of the Royal Society Interface* 9, 3108-3117.

Thorpe, C.T., Udeze, C.P., Birch, H.L., Clegg, P.D., Screen, H.R.C., 2013. Capacity for sliding between tendon fascicles decreases with ageing in injury prone equine tendons: a possible mechanism for age-related tendinopathy? *European Cells and Material* 25, 48-60.

Reviewer comment: BUT, 'Further research should confirm the value of this technique for diagnostic purposes and pre-surgical planning' How will it help pre-surgical planning? - if you have effusion in the DFTS which you think is clinically significant and no detectable tendon or manica flexoria lesion determined using ultrasonography you are going to perform a comprehensive tenoscopic examination. If you have identified a lesion you are going to perform tenoscopy, unless the lesion has a poor prognosis. Why involve the client in additional costs?

Authors' response: The authors agree that the benefit of this technique is debatable, depending on the location of a lesion the contrast study may however indicate which recumbency is most appropriate for tenoscopy.

‘The majority of equine surgeons perform tenoscopy with the horse in lateral recumbency, with the affected limb uppermost. If, for example, the horse was found at surgery to have a medial border deep digital flexor tendon tear, this would be difficult to debride with the limb uppermost. With computed tomographic contrast tenography and the ability to determine lesion laterality, the horse could be positioned appropriately to facilitate the best surgical access and hence improve outcome. Future study should be directed at investigating this technique for the evaluation of pathologic specimens.’ (Agass et al., 2018, page 282).

Agass, R., Dixon, J., Fraser, B., 2017. Computed tomographic contrast tenography of the digital flexor tendon sheath of the equine limb. *Veterinary Radiology & Ultrasound* 59, 279-288.

Reviewer comment: Line 373 What evidence do you have for the very sweeping statement 'and has high potential for the prevention of tendon injury,'? If only it was that simple!

Authors' response: The sentence was adjusted with the phrase ‘high potential’ removed to ensure it sounds less sweeping (line 428).

Reviewer comment: Figure legends need to describe the orientation of the images. How do these images enhance the manuscript? It would be more useful to show examples of where a lesion could not be seen using conventional imaging but was seen with 'advanced imaging' or was not

seen on a non-contrast enhanced image but was seen on a contrast enhanced image - or at least you gained additional useful information from contrast enhancement.

Authors' response: The orientation of the images is now stated in the figure legends (lines 948; 954; 961, 968 and 987) and further images including contrast CT were added to the manuscript (Figure 1 + 4).